LWDM. Warm Dark Matter Galaxy Theory inAgreement with Observations.

Norma G. SANCHEZ
DR CNRS LERMA Observatoire de Paris

18th Paris Cosmology Colloquium Chalonge 2014 23-25 July 2014

Basement- ground Zero

Dark matter is the dominant component of Galaxies and is an essential ingredient to understand Galaxy properties and Galaxy formation

Dark matter and Galaxy Formation must be treated in an cosmological context

The nature (the type) of Dark Matter and the cosmological model need to be explicitated when discussing galaxies and galaxy formation

All the building of galaxy formation depends on

the nature of Dark Matter

CONTENTS

(I) **The Standard Model of the Universe Includes Inflation**

(II) THE NATURE OF DARK MATTER IN GALAXIES from Theory and Observations: Warm (keV scale) DM

(III) NEW: THE ESSENTIAL ROLE OF QUANTUM PHYSICS IN WDM GALAXIES:
Semiclassical framework: Analytical Results and Numerical (including analytical) Results
Observed Galaxy cores and structures from Fermionic WDM and more results.

(IV) NEW: The generic Galaxy types and properties from a same physical framework: From quantum (compact, dwarfs) to classical (dilute, large) galaxies. Equation of state

HIGHLIGHTS

(I)The Effective (Ginsburg-Landau) Theory of Inflation

PREDICTIONS :

The Primordial Cosmic Banana: non-zero amount of primordial gravitons. And Forecasts for CMB exps.

(II) : TURNING POINT IN THE DARK MATTER PROBLEM: DARK MATTER IN GALAXIES from Theory and Observations: Warm (keV scale) dark matter

Physical Clarification and Simplification

GALAXY FORMATION AND EVOLUTION IN AGREEMENT WITH OBSERVATIONS

naturally re-insert in COSMOLOGY (LWDM)

Analytical Results and Numerical

UPDATE and CLARIFICATIONS

LCDM agrees with CMB + LSS BUT NOT with SSS (GALAXIES)

LWDM agrees with CMB + LSS + SSS (GALAXIES)

The Standard Model of the Universe is LWDM
GR, Newtonian Gravity , FT, QFT

sentences like « CMB confirms the LCDM model í   »

Must be completed: in large scales or updated: CMB confirms the LWDM model in large scales

NEW: Gravity and Quantum Mechanics in Galaxies
Newton, Fermi and Dirac meet together in Galaxies because of keV WDM

NEW RESULTS

FERMIONIC QUANTUM WDM and GRAVITATION DETERMINE THE OBSERVED PHYSICAL GALAXY PROPERTIES

-> Dark matter (DM) is the main component of galaxies. Quantum mechanics is a cornerstone of physics from microscopic to macroscopic systems as quantum liquids He^3, white dwarf stars and neutron stars.

-> NEW: Quantum mechanics is also responsible of galaxy structures at the kpc scales and below: near the galaxy center, below 10 - 100 pc, the DM quantum effects are important for warm DM (WDM), that is for DM particles with masses in the keV scale. DdVS (New Astronomy 2013) dVS PRD 2013, dVSS MNRAS to appear, dVS 2014

-> A new approach to galaxy structure with results in remarkable agreement with observations:

(i) Dwarf galaxies turn to be quantum macroscopic objects for WDM supported against gravity by the WDM fermion pressure

(ii) Theoretical analytic framework based on Thomas-Fermi approach determine galaxy structure from the most compact dwarf galaxies to the largest dilute galaxies (spirals, ellipticals).

The obtained galaxy mass, halo radius, phase-space density, velocity dispersion, are fully consistent with observations.

(iii) Interestingly enough, a minimal galaxy mass and minimal velocity dispersion are found for DM dominated objects, which in turn imply an universal minimal mass

$m\_min = 1.9$ keV for the WDM particle.

- **OBSERVED GALAXY CORES** vs CDM CUSPS and WDM CORES-

É **Well established sets of astronomical observations show that the DM galaxy density profiles are cored,** that is, profiles which are flat at the center.

On the contrary, **N-body CDM simulations exhibit cusped density profiles**, with a typical 1/r cusped behaviour near the galaxy center r = 0.

Classical Physics **N-body WDM simulations** exhibit cores but with sizes much smaller than the observed cores.

We have recently developped a new approach to this problem thanks to **Quantum Mechanics.**

É **Fermions** always provide a non vanishing **pressure of quantum nature** due to the combined action of the Pauli exclusion principle and Heisenberg uncertainty principle.

É **Quantum effects for WDM fermions <u>rule out</u> the presence of galaxy cusps for WDM and <u>enlarge</u> the classical core sizes because their <u>repulsive and non-local</u> nature extend well beyond the small pc scales.**

É **Smoothing the density profile at the central regions has an effect on the whole**

2014 DARK MATTER UPDATE

É **THERE IS NO CUSP/CORE problem:**

É **Observed Galaxy profiles are cored.**
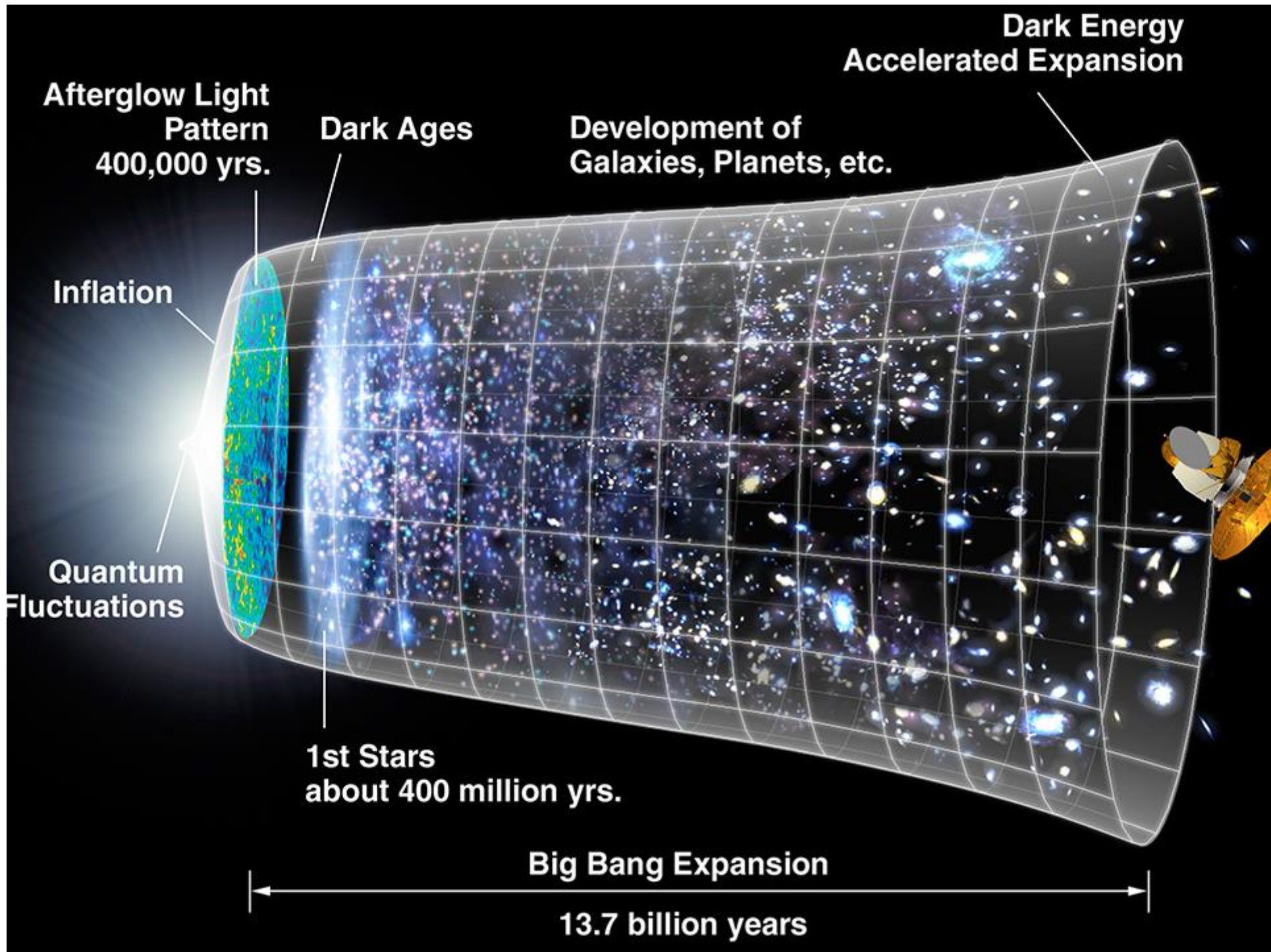
É **WDM Galaxy density profiles are cored**

É **THERE IS NO satellite problem**

É **WDM abundance of structures agrees with observations**

É In addition, these are not fundamental problems.

NO DM WIMPS, NO DM annhilation,

NO DM axions

From WMAP9 to New CMB data

Understanding the direction in which data are pointing:

É Our PREDICTIONS for Planck:

É **Standard Model of the Universe**

É **Standard Single field Inflation**

É **NO RUNNING of the Primordial Spectral Index**

É **NO Primordial NON GAUSSIANITY**

É N_{eff} **neutrinos : --> Besides meV active neutrinos:**

É **1 or 2 eV sterile neutrinos**

É **Would opens the sterile neutrino Family:**

É **keV sterile neutrino óWDM-**

Sterile neutrinos and CMB fluctuations

CMB data give the effective number of neutrinos, N_{eff}.

N_{eff} is related in a subtle way to the number of active neutrinos (3) plus the number of sterile neutrinos.

Planck result: $N_{eff} = 3.5 \pm 0.5$ (95%;P+WP+highL+H_0+BAO)

Entropy conservation determines the contributions to N_{eff}.

WDM sterile neutrino contribution at recombination

$\Delta N^{WDM} = \left(\frac{T_d}{T_{rc}}\right)^4 = \left[\frac{g_{rc}}{g(T_d)}\right]^{4/3}$. At recombination $g_{rc} = 29/4$.

WDM decouples early at T_d beyond the Fermi scale

The number of UR degrees of freedom at decoupling $g(T_d)$ includes all SM particles and probably beyond.

$g_{SM} = 427/4$, $g_{MSSM} = 915/4$,

$\Delta N^{WDM}_{SM} = 0.02771\ldots$, $\Delta N^{WDM}_{MSSM} = 0.01003\ldots$

Too small to be measurable at present !

Conclusion: Planck results say nothing about WDM.

Besides, Planck results are **compatible** with one or two eV sterile neutrinos (see e. g. G. Steigman, 1303.0049).

Recent News on Cosmological Observables

Before 2013: Hubble constant $H_0 = 73.8 \pm 2.4 \frac{\mathrm{km}}{\mathrm{s}} \frac{1}{\mathrm{Mpc}}$ from direct observations of Cepheids by HST, $\Omega_m = 0.27 \pm 0.03$. A G Riess et al. ApJ 730, 119 (2011).

Planck 2013: $H_0 = 67.3 \pm 1.2 \frac{\mathrm{km}}{\mathrm{s}} \frac{1}{\mathrm{Mpc}}$. $\Omega_m = 0.32 \pm 0.02$.

Planck assumed here only three massless neutrinos and no sterile neutrinos ν_s.

There is today strong evidence for ν_s with $m_s \sim$ eV from short baseline experiments (reactors, MiniBoone, LSND).

Adding one ν_s yields:

$H_0 = 70 \pm 1.2 \frac{\mathrm{km}}{\mathrm{s}} \frac{1}{\mathrm{Mpc}}$. $\Omega_m = 0.30 \pm 0.01$ for $m_s = 0.4$ eV.

These values for H_0 and Ω_m are compatible with the direct astronomical measurements.

M. Wyman et al. PRL. 112, 051302 (2014), J. Hamann & J. Haserkamp, JCAP,10,044H (2013) R. Battye & A. Moss, PRL. 112. 051303 (2014), S. Gariazzo et al. JHEP 1311

Active and Sterile Neutrinos

Active neutrinos (e, muon and tau) participate of weak interactions. Sterile neutrinos do not.

Neutrinos are characterized by their masses and mixing angles. Neutrinos can transform into each other.

Masses and mixing angles are obtained from nuclear (reactor) and particle physics experiments.
So far no theory for them.

WMAP9 and Planck gave $r < 0.11$ in tension with BICEP.

An extra sterile species is able to reconcile WMAP9 and Planck data with H_0 supernova data and the BICEP r.

Resulting sterile neutrino mass: $m_s \simeq 0.45$ eV

C. Dvorkin et al. arXiv:1403.8049, M. Archidiacono et al. arXiv:1404.1794, J. F. Zhang et al. 1403.7028.

Planck data analysis is faulty due to inadequate priors: zero active neutrino masses and no steriles.

Sterile Neutrinos ν

Rhenium and Tritium beta decay (MARE, KATRIN).
Theoretical analysis: H J de V, O. Moreno, E. Moya de Guerra, M. Ramón Medrano, N. Sánchez,
Nucl. Phys. B866, 177 (2013).

[Other possibility to detect a sterile ν_s: a precise measure of nucleus recoil in tritium beta decay.]

Conclusion: the empty slot of right-handed neutrinos in the Standard Model of particle physics can be filled by keV-scale sterile neutrinos describing the DM.

An appealing mass neutrino hierarchy appears:

- Active neutrino: $\sim$ mili eV
- Light sterile neutrino: $\sim$ eV
- Dark Matter: $\sim$ keV
- Unstable sterile neutrino: $\sim$ MeV....

Effective Theory of Inflation (ETI) confirmed by Planck

Quantity	ETI Prediction	Planck 2013
Spectral index $1 - n_s$	order $1/N = 0.02$	0.04
Running $dn_s/dlnk$	order $1/N^2 = 0.0004$	< 0.01
Non-Gaussianity f_{NL}	order $1/N = 0.02$	< 6
	ETI + WMAP+LSS	
tensor/scalar ratio r	r > 0.02	< 0.11 see BICEP
inflaton potential curvature $V''(0)$	$V''(0) < 0$	$V''(0) < 0$

ETI + WMAP+LSS means the MCMC analysis combining the ETI with WMAP and LSS data. Such analysis calls for an inflaton potential with negative curvature at horizon exit. The double well potential is favoured (new inflation). D. Boyanovsky, C. Destri, H. J. de Vega, N. G. Sanchez, arXiv:0901.0549, IJMPA 24, 3669-3864 (2009).

Two key observable numbers :
**associated to the primordial density and
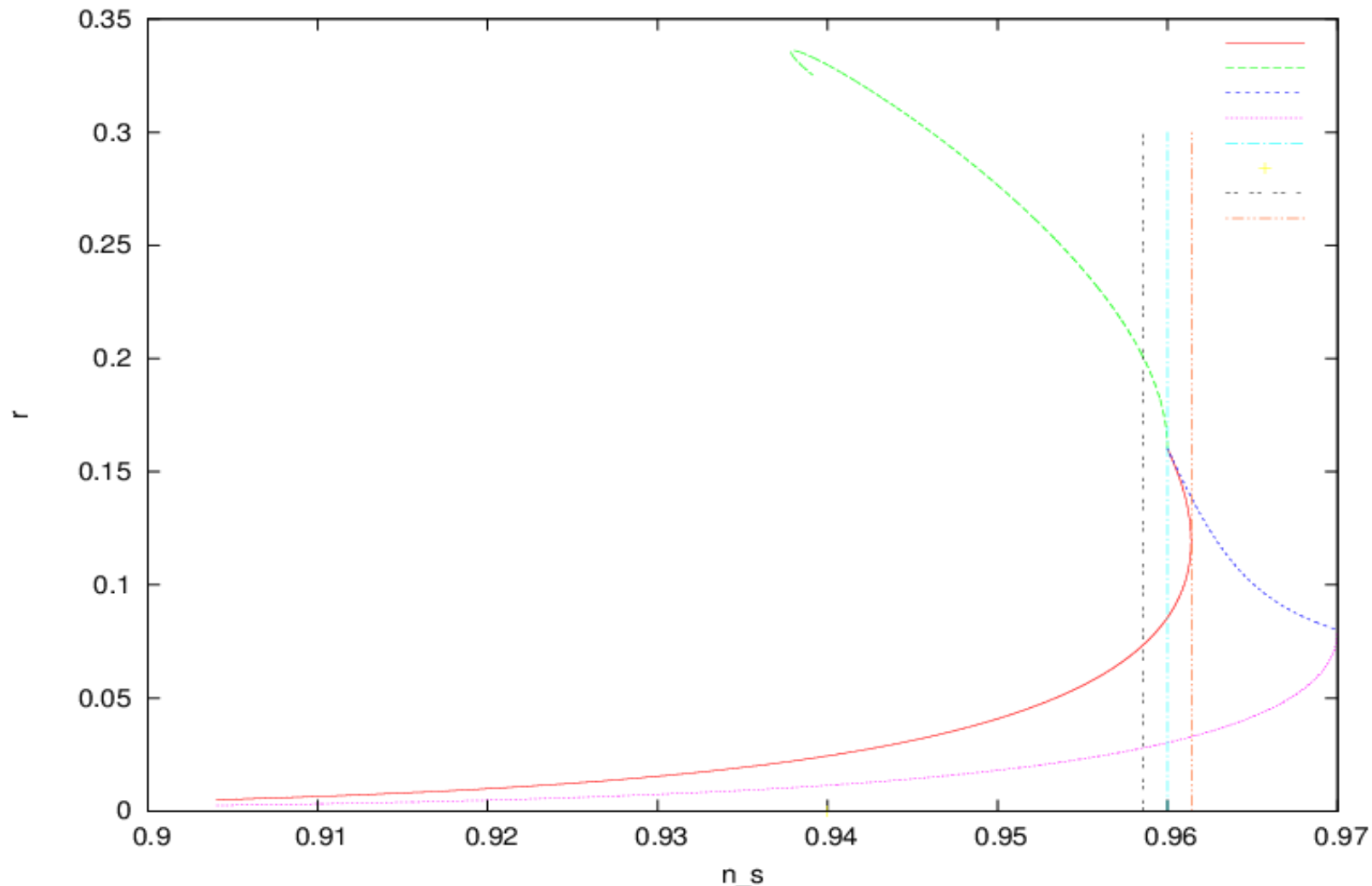primordial gravitons :**

$$n_s = 0.9608 \ , \quad r$$

PREDICTIONS

r > 0.021

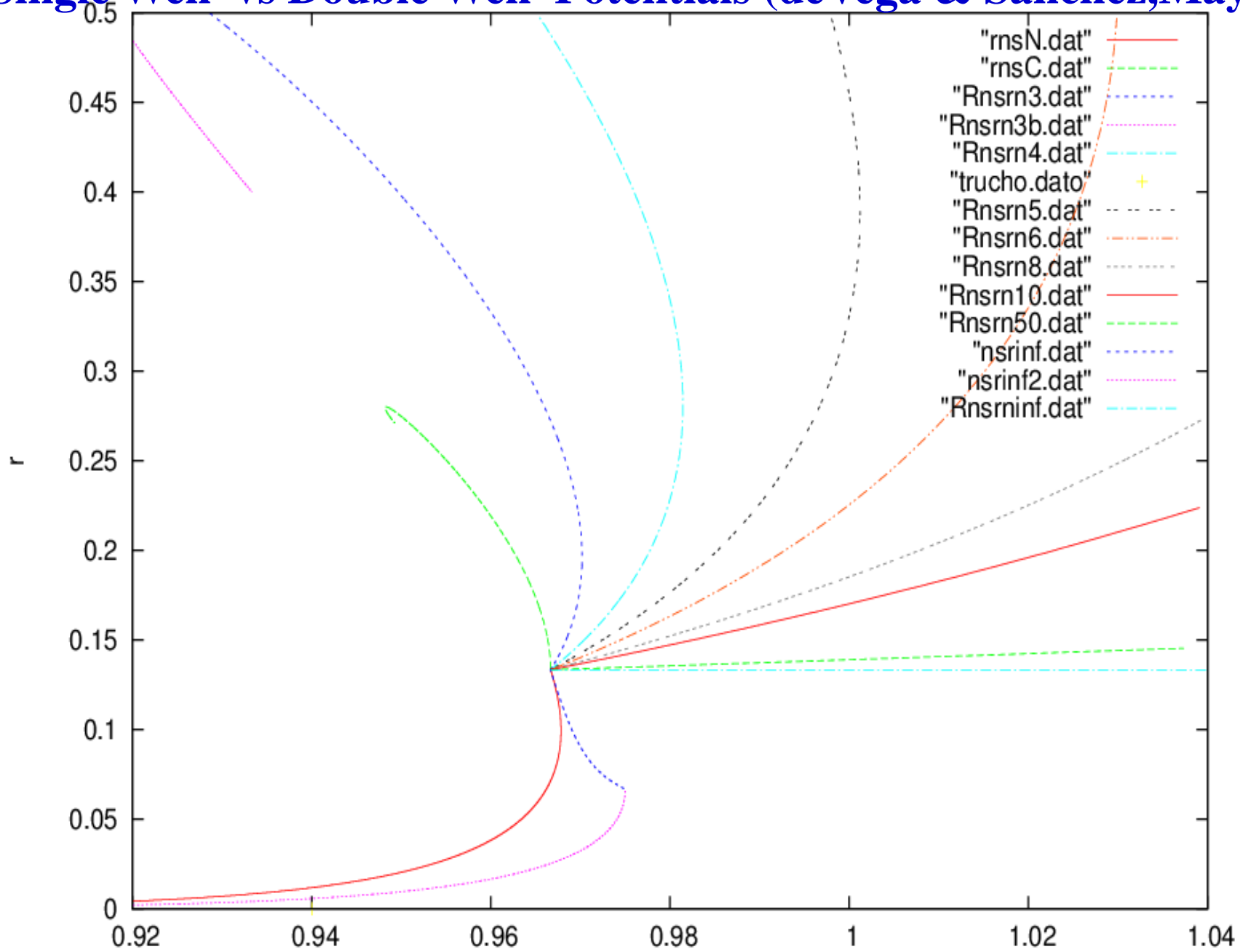**DdS: Destri, de Vega, Sanchez & from WMAP data
(PRD 2008)**

BICEP2 result 2014: r about 0.20-0.16

Single and Double Well Inflaton Potentials
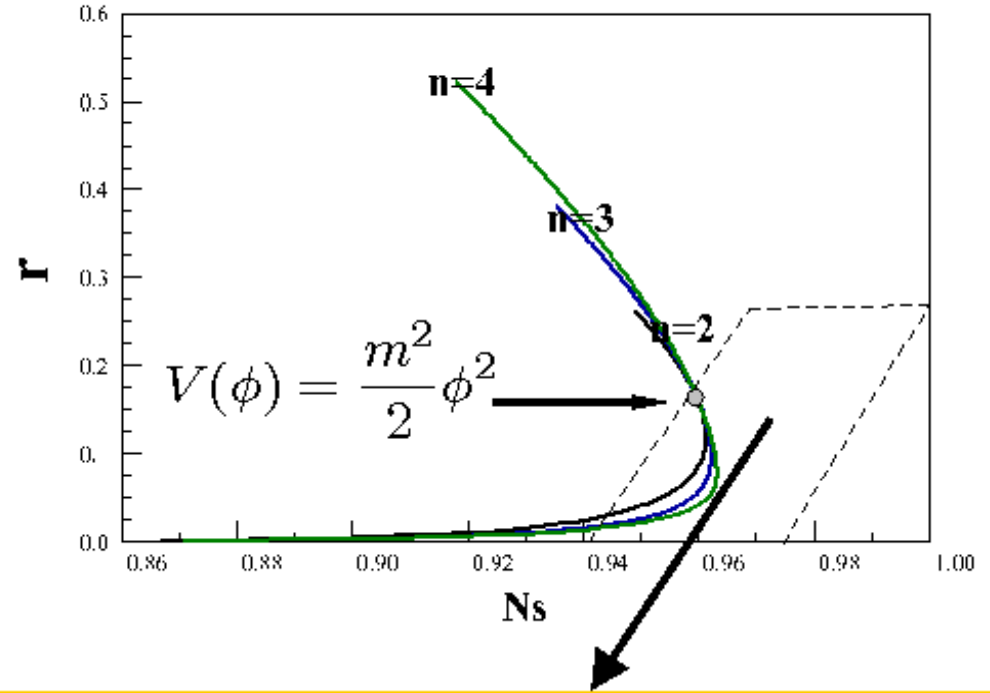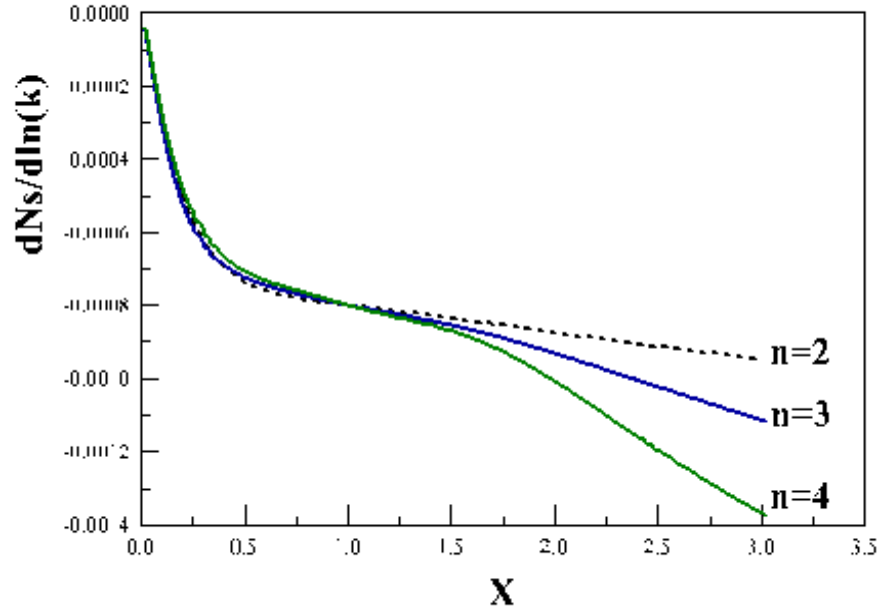

The cosmic banana for double well potentials (N=50) (de Vega, Sanchez, PRD 2006). Data 2014: $n_s = 0.96 \pm 0.014$.

Single Well vs Double Well Potentials (deVega & Sanchez,May 2014)

Legend:
- "rnsN.dat"
- "rnsC.dat"
- "Rnsrn3.dat"
- "Rnsrn3b.dat"
- "Rnsrn4.dat"
- "trucho.dato"
- "Rnsrn5.dat"
- "Rnsrn6.dat"
- "Rnsrn8.dat"
- "Rnsrn10.dat"
- "Rnsrn50.dat"
- "nsrinf.dat"
- "nsrinf2.dat"
- "Rnsrninf.dat"

1) New inflation (B.S.) Ne= 50 (change accordingly)
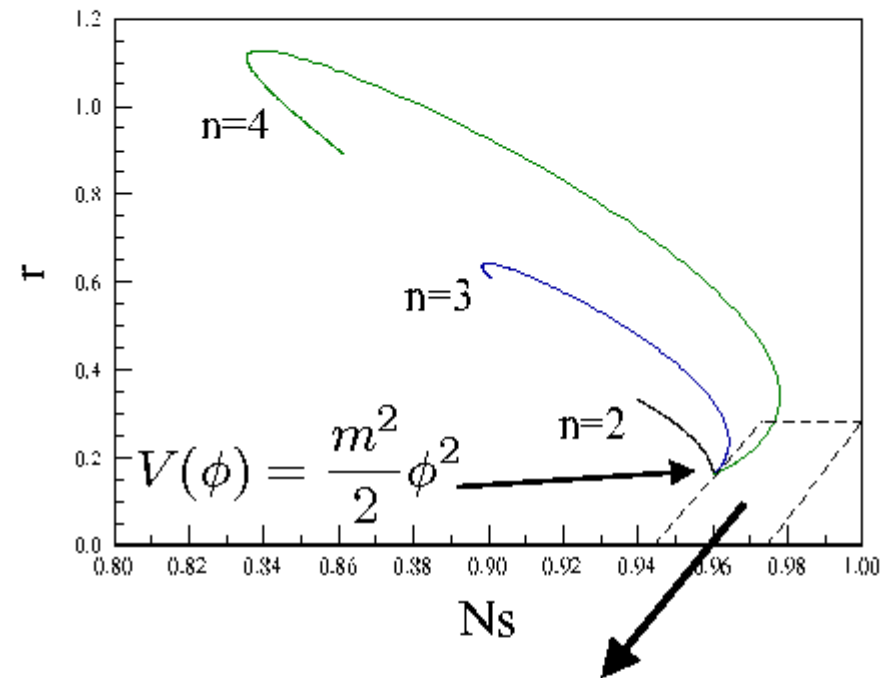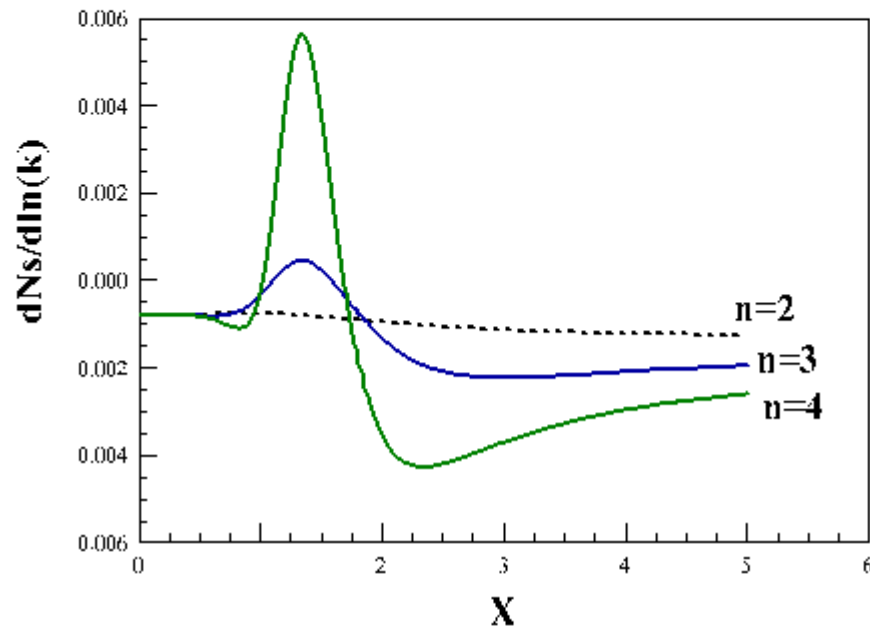

$$V(\phi) = \frac{m^2}{2}\phi^2$$

WMAP 3 marginalized region of r- n_s (95% CL)

* *Large region of consistency for small field New Inflation*

Boyanovsky, deVega, Ho & Sanchez , PRD 2007

2) Chaotic inflation

$$V(\phi) = \frac{m^2}{2}\phi^2$$

WMAP 3 marginalized region of r- ns (95% CL)

* Small region of consistency with WMAP 3

17

The Energy Scale of Inflation

Grand Unification Idea (GUT)

- Renormalization group running of electromagnetic, weak and strong couplings shows that they all meet at $E_{GUT} \simeq 2 \times 10^{16}$ GeV

- Neutrino masses are explained by the see-saw mechanism: $m_\nu \sim \frac{M_{\text{Fermi}}^2}{M_R}$ with $M_R \sim 10^{16}$ GeV.

- Inflation energy scale: $M \simeq 10^{16}$ GeV.

Conclusion: the GUT energy scale appears in at least three independent ways.

Moreover, moduli potentials: $V_{moduli} = M_{\text{SUSY}}^4 \, v \left(\frac{\phi}{M_{Pl}} \right)$
ressemble inflation potentials provided $M_{\text{SUSY}} \sim 10^{16}$ GeV.
First observation of SUSY in nature??

Large Hadron Collider - LHC-

The results are completely in line with the Standard Model.

No evidence of SUSY at LHC

õSupersymmetry may not be dead but these latest results have certainly put it into hospital."

(Prof Chris Parkes, spokesperson for the UK Participation in the LHCb experiment)
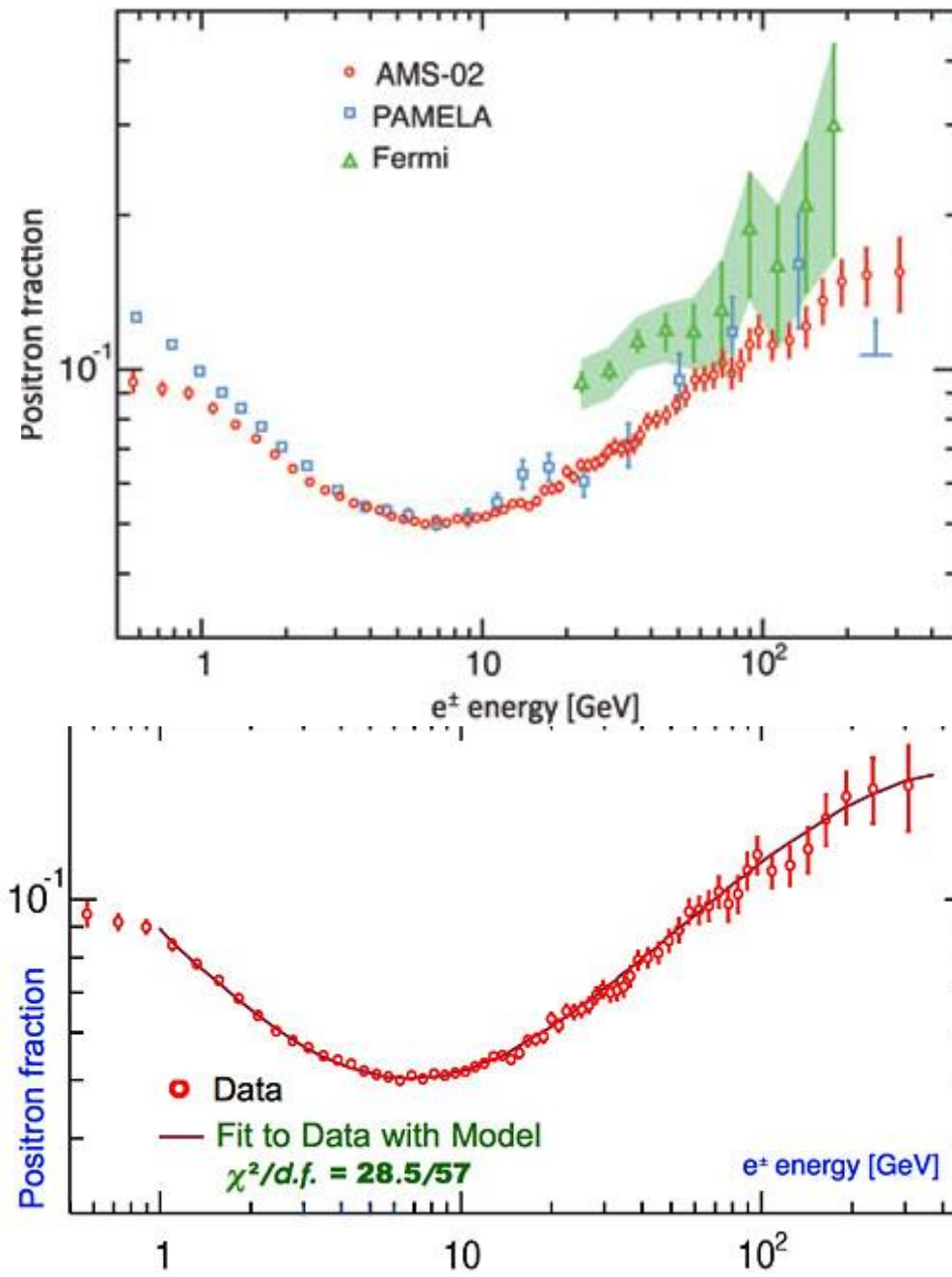
➔Does Not support wimps -CDM-

(In agreement with all dedicated wimp experiments at work from more than 20 years which have not found any wimpøs signal) **õSo far researchers who are racing to find evidence of so called "new physics", ie non-standard models, have run into a series of dead endsö.**

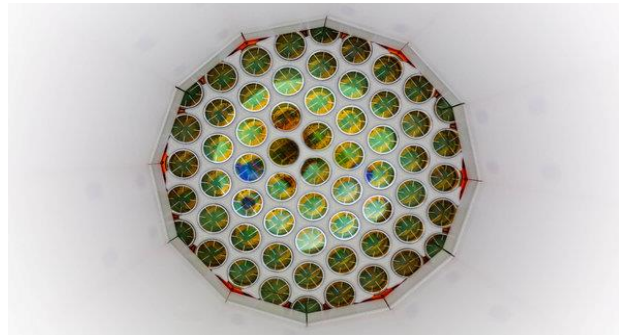# ANTIMATTER IN SPACE - AMS on board ISS Alpha Magnet Spectrometer

NASA

NASA

Positron excess in cosmic rays are not related to DM physics but to astrophysical sources and astrophysical mechanisms and can be explained by them

LUX Large Underground Xenon Detector
30 October 2013 and beyond

Dark Matter Experiment Has Detected Nothing, Researchers Say Proudly

É **They found no sign of WIMPS signals.**
   beyond the expected background noise.

É The experiment did so at far better sensitivities
   than any such experiment before it.

É Why No Experimental Detection of the DM particle has been reached so far ?

É Because:

- É **All experimental searches for DM particles are dedicated to CDM: GeV wimps**

- É **While the DM particle mass is in the keV scale** .

- É Moreover, past, present and future reports of signals of such CDM experiments **cannot be due to DM** because of the same reason.

- É **The inconclusive signals in such experiments should be originated by phenomena of other kinds.**

- É In addition, such signals contradict each other supporting the idea that they are **unrelated to any DM detection.**

Direct searches of CDM particles

All direct searches of wimps look for $m \gtrsim 1$ GeV.

Past, present and future reports of signals in such wimp experiments cannot be due to DM detection because the DM particle mass is in the keV scale.

The inconclusive signals in such experiments should be originated by other kinds of phenomena.

Contradictions between supposed detection signals in DAMA, CDMS-II, CoGeNT, CRESST, XENON100.

CONCLUSION: These signals are unrelated to DM.

e^+ and $\bar{p}$ excess in cosmic rays reported by Pamela and Fermi may be explained by astrophysics: P. L. Biermann et al. PRL (2009), P. Blasi, P. D. Serpico PRL (2009).

AMS02: precise measure of the positron fraction in Galactic cosmic rays (CR) (PRL 2013) that increases with energy. Blum, Katz & Waxman (arXiv:1305.1324) show that this is consistent with positron production by the collision of high energy primary CR with the interstellar medium.

WDM properties

WDM is characterized by

- its initial power spectrum cutted off for scales below ~ 50 kpc. Thus, structures are not formed in WDM for scales below ~ 50 kpc.

- its initial velocity dispersion. However, this is negligible for $z < 20$ where the non-linear regime starts.

- Classical N-body simulations break down at small distances ($\sim$ pc). Need of quantum calculations to find WDM cores.

Structure formation is hierarchical in CDM.

WDM simulations show in addition top-hat structure formation at large scales and low densities but hierarchical structure formation remains dominant.

Sterile neutrino models

- DW: Dodelson-Widrow model (1994) sterile neutrinos produced by non-resonant mixing from active neutrinos.

- Shi-Fuller model (1998) sterile neutrinos produced by resonant mixing from active neutrinos.

- νMSM model (2005) sterile neutrinos produced by a Yukawa coupling from a real scalar χ.

- Models based on: Froggatt-Nielsen mechanism, flavor symmetries, see-saw mechanisms and several variations of it, left-right symmetries and others. Review by A Merle (2013).

WDM particles in the first 3 models behave primordially just as if their masses were different (FD = thermal fermions):

$$\frac{m_{DW}}{\text{keV}} \simeq 2.85 \left(\frac{m_{FD}}{\text{keV}}\right)^{\frac{4}{3}}, \ m_{SF} \simeq 2.55 \, m_{FD}, \ m_{\nu\text{MSM}} \simeq 1.9 \, m_{FD}.$$

H J de Vega, N Sanchez, Warm Dark Matter cosmological fluctuations, Phys. Rev. D85, 043516 and 043517 (2012).

Detection of a 3.56 keV X-ray line in galaxy clusters

E.Bulbul et al. ApJ 789, 23 (2014) reported the detection of a new X-ray line in galaxy clusters that may be originated by the decay of a 7.1 keV sterile neutrino.
Sterile neutrinos remain out of thermal equilibrium today.

From the conversion formulas, a 7.1 keV DW sterile neutrino behaves as a 1.99 keV thermal relic and a 7.1 keV SF sterile neutrino behaves as a 2.8 keV thermal relic.

Besides, a 7.1 keV SF sterile neutrino with lepton asymmetry yields similar results (K Abazajian, 2014).

WDM thermal relics with thermal mass near 2 keV provide correct small scale structure formation.

Therefore, a 7.1 keV sterile neutrino may be the dark matter particle.

Confirmation of the detection and identification of the 3.56 keV X-ray line from Astro-H is awaited for 2015 !

Structure Formation in the Universe

Structures in the Universe as galaxies and cluster of galaxies form out of the small primordial quantum fluctuations originated by inflation just after the big-bang.

These linear small primordial fluctuations grow due to gravitational unstabilities (Jeans) and then classicalize.

Structures form through non-linear gravitational evolution. Hierarchical formation starts from small scales first.

N-body CDM simulations fail to produce the observed structures for small scales less than some kpc.

Both N-body WDM and CDM simulations yield identical and correct structures for scales larger than some kpc.

WDM predicts correct structures for small scales (below kpc) when its quantum nature is taken into account.

Primordial power $P(k)$: first ingredient in galaxy formation.

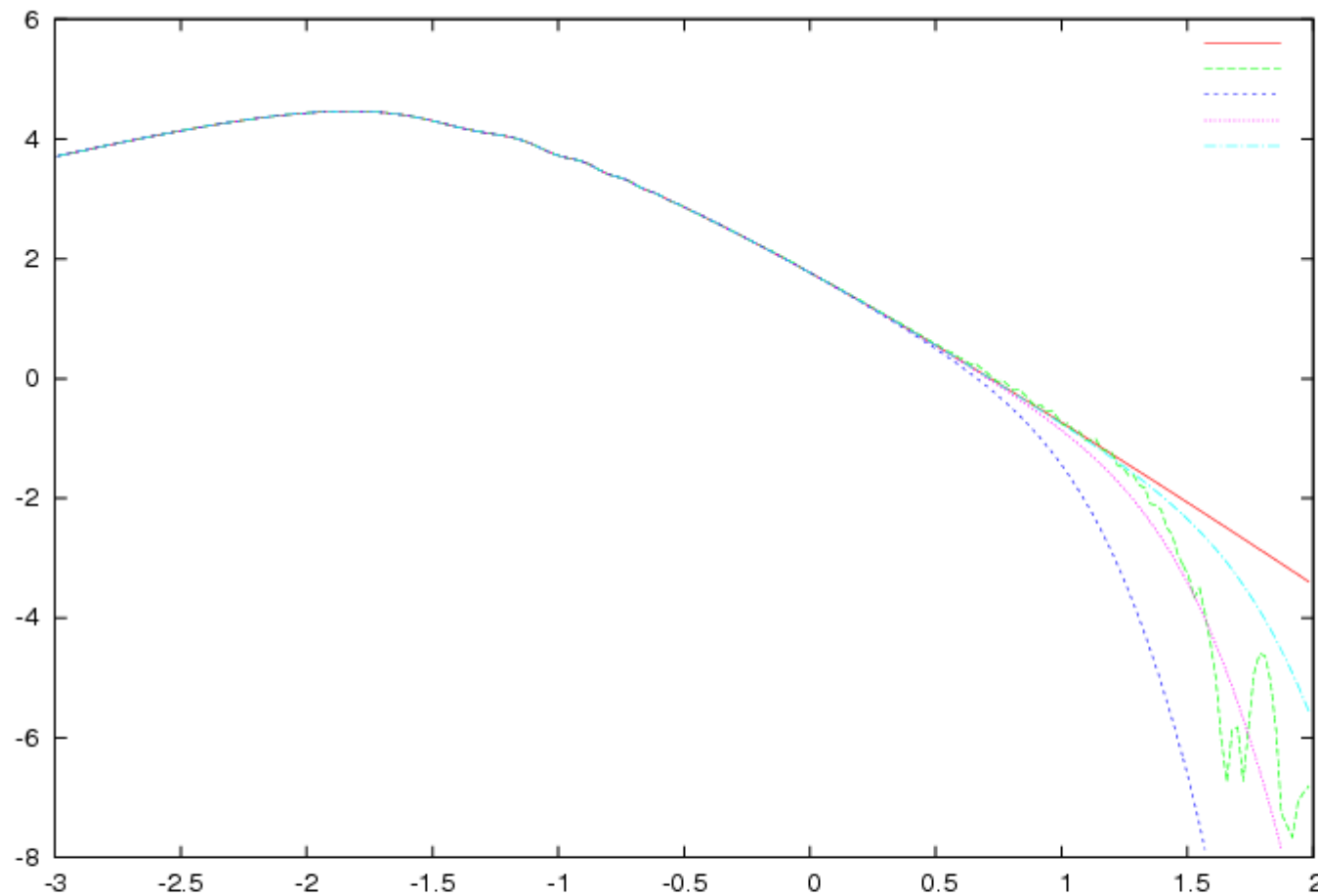# Linear primordial power today $P(k)$ vs. k Mpc h
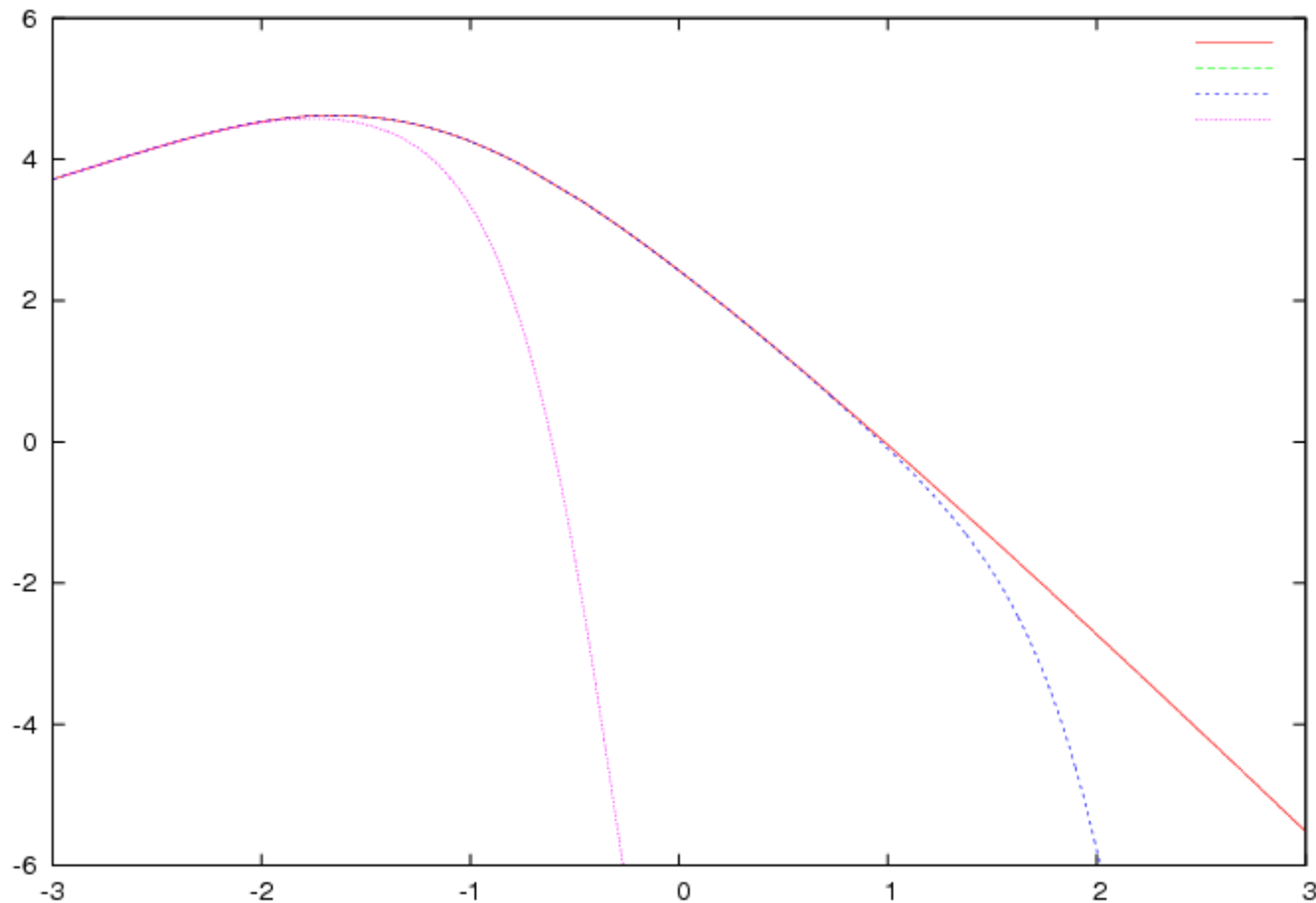
$\log_{10} P(k)$ vs. $\log_{10}[k \text{ Mpc } h]$ for **WIMPS**, **1 keV** DM particles and **10 eV** DM particles. $P(k) = P_0 \, k^{n_s} \, T^2(k)$.

$P(k)$ cutted for **1 keV** DM particles on scales $\lesssim 100$ kpc.

Transfer function in the MD era from Gilbert integral eq.

Linear primordial power today $P(k)$ vs. k Mpc h

$\log_{10} P(k)$ vs. $\log_{10}[k \text{ Mpc } h]$ for CDM, 1 keV, 2 keV, light-blue 4 keV DM particles decoupling in equil, and 1 keV sterile neutrinos. WDM cuts $P(k)$ on small scales $r \lesssim 100 \, (\text{keV}/m)^{4/3}$ kpc. CDM and WDM identical for CMB.

WDM Primordial Power Spectrum

The WDM Primordial Power Spectrum is obtained solving the linear Boltzmann-Vlasov equations.

We define the transfer function ratio $T^2(k) \equiv \frac{\Delta^2_{wdm}(k)}{\Delta^2_{cdm}(k)}$

Reproduced by the analytic formula $T^2(k) = \left[1 + \left(\frac{k}{\kappa}\right)^a\right]^{-b}$

a and b are independent of the WDM particle mass m.

κ scales with m. In our best fit:

$$a = 2.304 \,, \quad b = 4.478 \,, \quad \kappa = 14.6 \; (m_{FD}/\text{keV})^{1.12} \; h/\text{Mpc}$$

At the wavenumber $k_{1/2}$: $T^2(k_{1/2}) = 1/2$ and

$$k_{1/2} = 6.72 \; (m_{FD}/\text{keV})^{1.12} \; h/\text{Mpc}$$

The characteristic length scale is

$$l_{1/2} = 1/k_{1/2} = 207 \text{ kpc} \; (\text{keV}/m_{FD})^{1.12}$$

This scale reproduces the sizes of the DM galaxy cores when the WDM mass is in the keV scale !!

The Mass function

The differential mass function gives the number of isolated bounded structures with mass between M and $M + dM$: (Press-Schechter)

$$\frac{dN}{dM} = -\frac{2\,\delta_c}{\sqrt{2\,\pi}\,\sigma^2(M,z)}\,\frac{\rho_M(z)}{M^2}\,\frac{d\sigma(M,z)}{d\ln M}\,e^{-\delta_c^2/[2\,\sigma^2(M,z)]},$$

$\delta_c = 1.686\ldots$: linear estimate for collapse from the spherical model.

$\sigma(M,z)$ is constant for WDM for small scales: small objects (galaxies) formation is suppresed in WDM in comparison with CDM.

$$\sigma(M,z) = \frac{g(z)}{z+1}\,\sigma(M,0)$$

$g(z)$: takes into account the effect of the cosmological constant, $g(0) = 0.76$, $g(\infty) = 1$

Relative overdensity D(R) and Press-Schechter approach

The number of isolated bounded structures with mass between M and $M + dM$: (Press-Schechter)

$$\frac{dN}{dM} = -\frac{2\,\delta_c}{\sqrt{2\pi}\,\sigma^2(M,z)}\,\frac{\rho_M(z)}{M^2}\,\frac{d\sigma(M,z)}{d\ln M}\,e^{-\delta_c^2/[2\,\sigma^2(M,z)]},\ \ \delta_c = 1.686\ldots$$

$\sigma(M,z)$ is constant for WDM for small scales: small objects formation is suppressed in WDM in comparison with CDM.

Computing dN/dM in WDM shows that small scale structure suppression with respect to CDM increases with z. H. J. de Vega, N. G. Sanchez, arXiv:1308.1109, Phys.Rev.D

It is therefore important to compare the observations at $z > 1$ with the theoretical predictions:

Menci et al. ApJ 2013, Nierenberg et al. ApJ 2013,

Conclusion: WDM reproduces the observed small scale structures better than CDM for redshifts up to eight where observations are available.

Redshift dependence and Relative overdensity D(R)

$$\sigma(M, z) = \frac{g(z)}{z+1}\, \sigma(M, 0) \quad \text{during the MD/}\Lambda \text{ dominated era.}$$

$g(z)$: the effect of the cosmological constant. $g(z)$ is a hypergeometric function $_2F_1$, $g(0) = 0.76$, $g(\infty) = 1$

We introduce the relative overdensity: $D(R) \equiv \frac{\sigma^2_{WDM}(R,z)}{\sigma^2_{CDM}(R,z)}$

(z dependence cancels out).

Characteristic scale below which structures are suppresed in WDM compared with CDM: $R_{1/2}$ where $D(R_{1/2}) = 1/2$,

$$R_{1/2} = 73.1\, \frac{\text{kpc}}{h}\, \left(\frac{\text{keV}}{m_{FD}}\right)^{1.45}$$
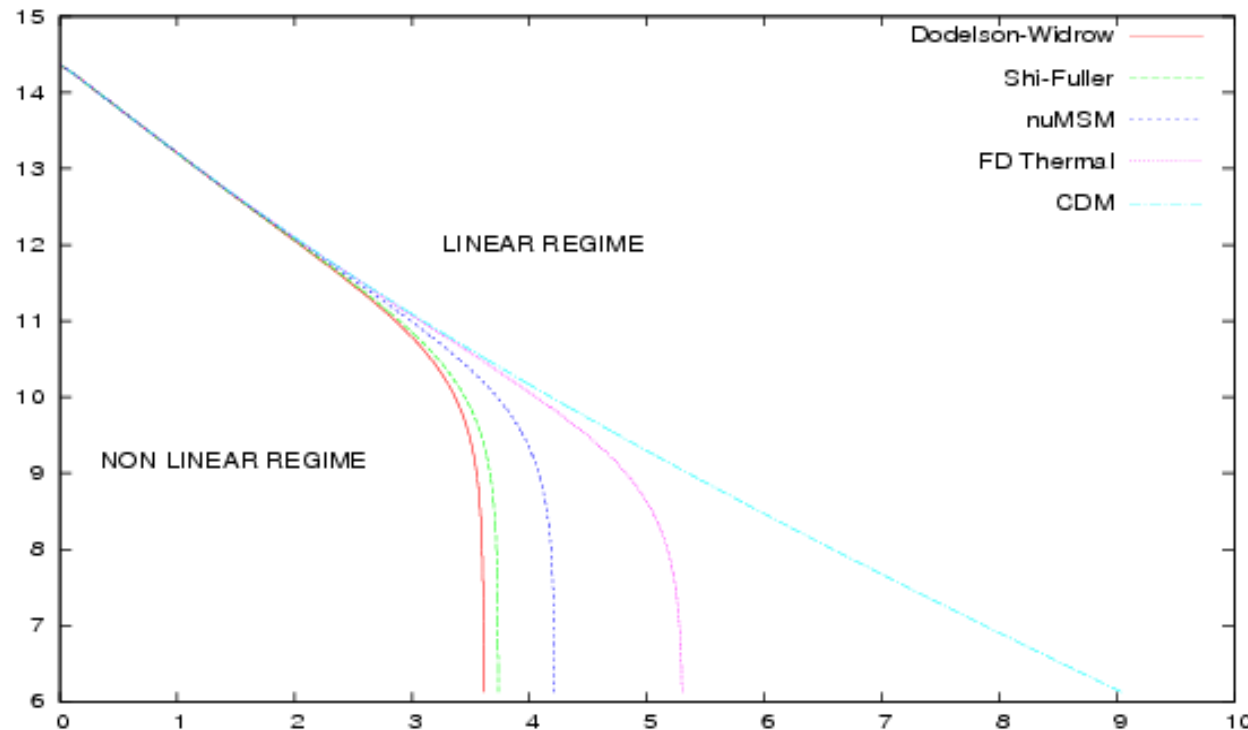
$D(R)$ can be reproduced by the simple formula:

$$D(R) = \left[1 + \left(2^{1/\beta} - 1\right) \left(\frac{R_{1/2}}{R}\right)^{\alpha}\right]^{-\beta}$$

$$\alpha \simeq 2.2 \quad , \quad \beta \simeq 0.17 \quad , \quad 2^{1/\beta} - 1 \simeq 58$$

Linear and non-linear regimes in z and R

$\sigma^2(R, z) \sim 1$: borderline between linear and non-linear regimes. Objects (galaxies) of scale R and mass $\sim R^3$ start to form when this scale becomes non-linear.
Smaller objects can form earlier.

$\sigma^2(M, z) = 1$ in the z, $\log[h\, M/M_\odot]$ plane for $m = 2.5$ keV in four different WDM models and in CDM.

The constant surface density in DM and luminous galax

The Surface density for dark matter (DM) halos and for luminous matter galaxies defined as: $\mu_{0D} \equiv r_0 \, \rho_0$,

r_0 = halo core radius, ρ_0 = central density for DM galaxies

$$\mu_{0D} \simeq 120 \, \frac{M_\odot}{\text{pc}^2} = 5500 \, (\text{MeV})^3 = (17.6 \, \text{Mev})^3$$

5 kpc $< r_0 <$ 100 kpc. For luminous galaxies $\rho_0 = \rho(r_0)$. Donato et al. 09, Gentile et al. 09.[$\mu_{0D} = g$ in the surface].

Universal value for μ_{0D}: independent of galaxy luminosity for a large number of galactic systems (spirals, dwarf irregular and spheroidals, elliptics) spanning over 14 magnitudes in luminosity and of different Hubble types.

Similar values $\mu_{0D} \simeq 80 \, \frac{M_\odot}{\text{pc}^2}$ in interstellar molecular clouds of size r_0 of different type and composition over scales $0.001 \, \text{pc} < r_0 < 100$ pc (Larson laws, 1981).

WARM DARK MATTER REPRODUCE

→OBSERVED GALAXY DENSITIES
AND VELOCITY DISPERSIONS

→SOLVES the OVERABUNDANCE (õsatellite)
PROBLEM

->OBSERVED SURFACE DENSITY VALUES OF
DARK MATTER DOMINATED GALAXIES

→OBSERVED GALAXY
CORED DENSITY PROFILES : QUANTUM
MECHANICS

Quantum Bounds on Fermionic Dark Matter

The Pauli principle gives the upper bound to the phase space distribution function of spin-$\frac{1}{2}$ particles of mass m:

$$f(\vec{r}, \vec{p}) \leq 2$$

The DM mass density is given by:

$$\rho(\vec{r}) = m \int d^3p \, \frac{f(\vec{r}, \vec{p})}{(2\pi\hbar)^3} = \frac{m^4}{2\hbar^3} \, \sigma^3(\vec{r}) \, \bar{f}(\vec{r}) \, K \,,$$

where:

$\bar{f}(\vec{r})$ is the $\vec{p}$−average of $f(\vec{r}, \vec{p})$ over a volume $m^3 \sigma^3(\vec{r})$,

$\sigma(\vec{r})$ is the DM velocity dispersion, $\sigma^2(\vec{r}) \equiv <v^2(\vec{r})>/3$

$K \sim 1$ a pure number.

The Pauli bound $\bar{f}(\vec{r}) \leq 2$ yields: $Q(\vec{r}) \equiv \frac{\rho(\vec{r})}{\sigma^3(\vec{r})} \leq K \frac{m^4}{\hbar^3}$

This is an absolute quantum upper bound on $Q(\vec{r})$ due to quantum physics, namely the Pauli principle.
$Q(\vec{r})$ can **never** take values larger than $K \, m^4/\hbar^3$.
In the classical limit $\hbar \to 0$ and the bound disappears.

Dwarf galaxies as quantum objects

de Broglie wavelength of DM particles $\lambda_{dB} = \frac{\hbar}{m\,\sigma}$

d = mean distance between particles,
σ = DM mean velocity

$$d = \left(\frac{m}{\rho}\right)^{\frac{1}{3}} \quad , \qquad Q = \rho/\sigma^3 \quad , \qquad Q = \text{phase space density.}$$

ratio: $\qquad \mathcal{R} = \frac{\lambda_{dB}}{d} = \hbar\left(\frac{Q}{m^4}\right)^{\frac{1}{3}}$

Observed values: $2 \times 10^{-3} < \mathcal{R}\left(\frac{m}{\text{keV}}\right)^{\frac{1}{3}} < 1.4$

The larger $\mathcal{R}$ is for ultracompact dwarfs.
The smaller $\mathcal{R}$ is for big spirals.

$\mathcal{R}$ near unity (or above) means a QUANTUM OBJECT.

Observations alone show that compact dwarf galaxies are quantum objects (for WDM).

Galaxy	$\dfrac{r_h}{\mathrm{pc}}$	$\dfrac{\sigma}{\frac{\mathrm{km}}{\mathrm{s}}}$	$\dfrac{\hbar^{\frac{3}{2}}\sqrt{Q_h}}{(\mathrm{keV})^2}$	$\rho(0)/\dfrac{M_\odot}{(\mathrm{pc})^3}$	$\dfrac{M_h}{10^6\,M_\odot}$
Willman 1	19	4	0.85	6.3	0.029
Segue 1	48	4	1.3	2.5	1.93
Leo IV	400	3.3	0.2	.19	200
Canis Venatici II	245	4.6	0.2	0.49	4.8
Coma-Berenices	123	4.6	0.42	2.09	0.14
Leo II	320	6.6	0.093	0.34	36.6
Leo T	170	7.8	0.12	0.79	12.9
Hercules	387	5.1	0.078	0.1	25.1
Carina	424	6.4	0.075	0.15	32.2
Ursa Major I	504	7.6	0.066	0.25	33.2
Draco	305	10.1	0.06	0.5	26.5
Leo I	518	9	0.048	0.22	96
Sculptor	480	9	0.05	0.25	78.8
Boötes I	362	9	0.058	0.38	43.2
Canis Venatici I	1220	7.6	0.037	0.08	344
Sextans	1290	7.1	0.021	0.02	116
Ursa Minor	750	11.5	0.028	0.16	193
Fornax	1730	10.7	0.016	0.053	1750
NGC 185	450	31	0.033	4.09	975
NGC 855	1063	58	0.01	2.64	8340
Small Spiral	5100	40.7	0.0018	0.029	6900
NGC 4478	1890	147	0.003	3.7	6.55×10^4
Medium Spiral	1.9×10^4	76.2	3.7×10^{-4}	0.0076	1.01×10^5
NGC 731	6160	163	9.27×10^{-4}	0.47	2.87×10^5
NGC 3853	5220	198	8.8×10^{-4}	0.77	2.87×10^5
NGC 499	7700	274	5.9×10^{-4}	0.91	1.09×10^6
Large Spiral	5.9×10^4	125	0.96×10^{-4}	2.3×10^{-3}	$1. \times 10^6$

TABLE I: Observed values r_h, σ, $\sqrt{Q_h}$, $\rho(0)$ and M_h covering from ultracompact objects and

The quantum radius r_q for different kinds of DM

DM type	DM particle mass	r_q	
CDM	$1 - 100$ GeV	$1 - 10^4$ meters	in practice zero
WDM	$1 - 10$ keV	$0.1 - 1$ pc	compatible with observed cores
HDM	$1 - 10$ eV	kpc - Mpc	too big !

Self-gravitating Fermions in the Thomas-Fermi approach

WDM is non-relativistic in the MD era. A single DM halo in late stages of formation relaxes to a time-independent form especially in the interior.

Chemical potential: $\mu(r) = \mu_0 - m\,\phi(r)$, $\phi(r) =$ grav. pot.

Poisson's equation: $\frac{d^2\mu}{dr^2} + \frac{2}{r}\frac{d\mu}{dr} = -4\,\pi\,G\,m\,\rho(r)$

$\rho(0) =$ finite for fermions $\Longrightarrow \frac{d\mu}{dr}(0) = 0$.

Density $\rho(r)$ and pressure $P(r)$ in terms of the distribution function $f(E)$:

$$\rho(r) = \frac{m}{\pi^2\,\hbar^3}\int_0^\infty p^2\,dp\,f\big[\tfrac{p^2}{2m} - \mu(r)\big]$$

$$P(r) = \frac{1}{3\,\pi^2\,m\,\hbar^3}\int_0^\infty p^4\,dp\,f\big[\tfrac{p^2}{2m} - \mu(r)\big]$$

These are self-consistent non-linear Thomas-Fermi equations that determine $\mu(r)$.

WDM Thomas-Fermi equations

Self-consistent dimensionless Thomas-Fermi equation:

$$\frac{d^2\nu}{d\xi^2} + \frac{2}{\xi}\frac{d\nu}{d\xi} + I_2(\nu) = 0 \quad , \quad \nu'(0) = 0$$

Core size r_h of the halo defined as for Burkert profile:

$$\frac{\rho(r_h)}{\rho_0} = \frac{1}{4} \quad , \quad r_h = l_0\,\xi_h$$

Fermi-Dirac Phase-Space distribution function $f(E/T_0)$:

Contrasting the theoretical Thomas-Fermi solution with **galaxy data**, T_0 turns to be $10^{-3}\ ^oK < T_0 < 20\ ^oK$

colder = ultracompact, warmer = large spirals.
$T_0 \sim m\ <v^2>_{\text{observed}}$ for $m \sim 2$ keV.

All results are independent of any WDM particle physics model, they only follow from the gravitational interaction of the WDM particles and their fermionic nature.

Thomas-Fermi approximation: solutions

$$-M(R) = \frac{(3\,\pi)^2\,\hbar^6}{256\,G^3\,m^8\,R^3}\ \xi_0^5\ |\nu'(\xi_0)|$$

$$P(r) = \frac{\pi^{\frac{4}{3}}}{3}\,\hbar^2\,\left[\frac{\rho(0)}{\beta(\xi_0)\,m^4}\right]^{\frac{5}{3}}\int_0^\infty y^4\,dy\,\Psi\left(y^2 - \nu(\xi)\right)$$

L_0 and $M(R)$ turn to be of the order of the Jeans' length and the Jeans' mass, respectively.

The chemical potential at $r = 0$ fixed by the value of $Q(0)$.

Using observed values of $Q(0)$, we obtain halo radius $r_s \sim 0.1 - 10$ kpc, galaxy masses $10^5 - 10^7\,M_\odot$ and velocity dispersions, all consistent with the observations of dwarf galaxies.

The Thomas-Fermi approach gives realistic halo radii, larger than the quantum lower bound r_q, as expected.

Fermionic WDM treated quantum mechanically is able to reproduce the observed DM cores of galaxies.

Self-gravitating Fermions in the Thomas-Fermi approach

The Thomas-Fermi approach gives physical galaxy magnitudes: mass, halo radius, phase-space density and velocity dispersion fully compatible with observations from the largest spiral galaxies till the ultracompact dwarf galaxies for a WDM particle mass around 2 keV.

Compact dwarf galaxies are close to a degenerate WDM Fermi gas while large galaxies are classical WDM Boltzmann gases.

Fermionic WDM treated quantum mechanically is able to reproduce the observed galaxies.

C. Destri, H. J. de Vega, N. G. Sanchez, arXiv:1204.3090 to appear in New Astronomy. 'Quantum WDM fermions and gravitation determine the observed galaxy structures', arXiv:1301.1864.

RESULTS

All the obtained density profiles are cored.

The Core Sizes are in agreement with the observations

**from the compact galaxies where $r_h \sim 20$ pc till the
spiral and elliptical galaxies where $r_h \sim 0.2 - 60$ kpc.**

**The larger and positive is the chemical potential $\nu(0)$, the smaller is the core.
The minimal one arises in the degenerate case $\nu(0)$ --> to +infinity
(compact dwarf galaxies).
And
The Phase-space Density
The Galaxy halo Masses.**

**Agreement is found in all the range of galaxies
for a DM particle mass m around 2 keV.**

Error bars of the observational data are not shown but they are at least about 10-20 %.

Galaxy data vs. Thomas-Fermi

Mass, halo radius, velocity dispersion and central density from a broad variety of galaxies: ultracompact galaxies to giant spirals, Willman 1, Segue 1, Canis Venatici II, Coma-Berenices, Leo II, Leo T, Hercules, Carina, Ursa Major I, Draco, Leo I, Sculptor, Boötes, Canis Venatici I, Sextans, Ursa Minor, Fornax, NGC 185, NGC 855, NGC 4478, NGC 731, NGC 3853, NGC 499 and a large number of spiral galaxies.

Phase-Space distribution function $f(E/E_0)$: Fermi-Dirac ($F(x) = \frac{1}{e^x+1}$) and out of equilibrium sterile neutrinos give similar results.

E_0 = effective galaxy temperature (energy scale).

E_0 turns to be $10^{-3}\,{}^o$K $< E_0 < 50\,{}^o$K

colder = ultracompact, warmer = large spirals.

$E_0 \sim m\ <v^2>_{\text{observed}}$ for $m \sim 2$ keV.

Galaxy surface density

The surface density: $\Sigma_0 \equiv r_h \, \rho_0 \simeq 120 \; M_\odot/\text{pc}^2$,

takes nearly the same value for galactic systems (spirals, dwarf irregular and spheroidals, elliptics) spanning over 14 magnitudes in luminosity and over different Hubble types.

We take Σ_0 as physical scale to express the galaxy magnitudes in the Thomas-Fermi approach.

Dimensionless variables: $\xi, \; \nu(\xi)$.

$$r = l_0 \, \xi \quad, \quad \mu(r) = T_0 \, \nu(\xi) \quad, \quad \rho_0 \equiv \rho(0).$$

$T_0 = $ effective galaxy temperature, l_0 characteristic length.

From the Thomas-Fermi equations:

$$l_0 = \left(\frac{9\pi}{2^9}\right)^{\frac{1}{5}} \left(\frac{\hbar^6}{G^3 m^8}\right)^{\frac{1}{5}} \left[\frac{\xi_h \, I_2(\nu_0)}{\Sigma_0}\right]^{\frac{1}{5}} =$$

$$4.2557 \left[\xi_h \, I_2(\nu_0)\right]^{\frac{1}{5}} \left(\frac{2\,\text{keV}}{m}\right)^{\frac{8}{5}} \left(\frac{120\,M_\odot}{\Sigma_0 \text{pc}^2}\right)^{\frac{1}{5}} \text{pc}$$

$$I_n(\nu) \equiv (n+1) \int_0^\infty u^n \, du \; f(u^2 - \nu) \quad, \quad \nu_0 \equiv \nu(0)$$

Lower bound on the particle mass m

In the degenerate quantum limit $\nu_0 \to +\infty,\ T_0 \to 0$ the galaxy mass and halo radius take their minimum values

$$r_h^{min} = 11.3794 \left(\frac{2\,\mathrm{keV}}{m}\right)^{\frac{8}{5}} \left(\frac{120\ M_\odot}{\Sigma_0\ \mathrm{pc}^2}\right)^{\frac{1}{5}}\ \mathrm{pc}$$

$$M_h^{min} = 30998.7 \left(\frac{2\,\mathrm{keV}}{m}\right)^{\frac{16}{5}} \left(\frac{\Sigma_0\ \mathrm{pc}^2}{120\ M_\odot}\right)^{\frac{3}{5}}\ M_\odot$$

Observed halo masses must be larger or equal than M_h^{min}

From the minimum observed value of the halo mass M_h^{min} a lower bound for the WDM particle mass m follows

$$m \geq m_{min} \equiv 1.387\ \mathrm{keV} \left(\frac{10^5\ M_\odot}{M_h^{min}}\right)^{\frac{5}{16}} \left(\frac{\Sigma_0\ \mathrm{pc}^2}{120\ M_\odot}\right)^{\frac{3}{16}}$$
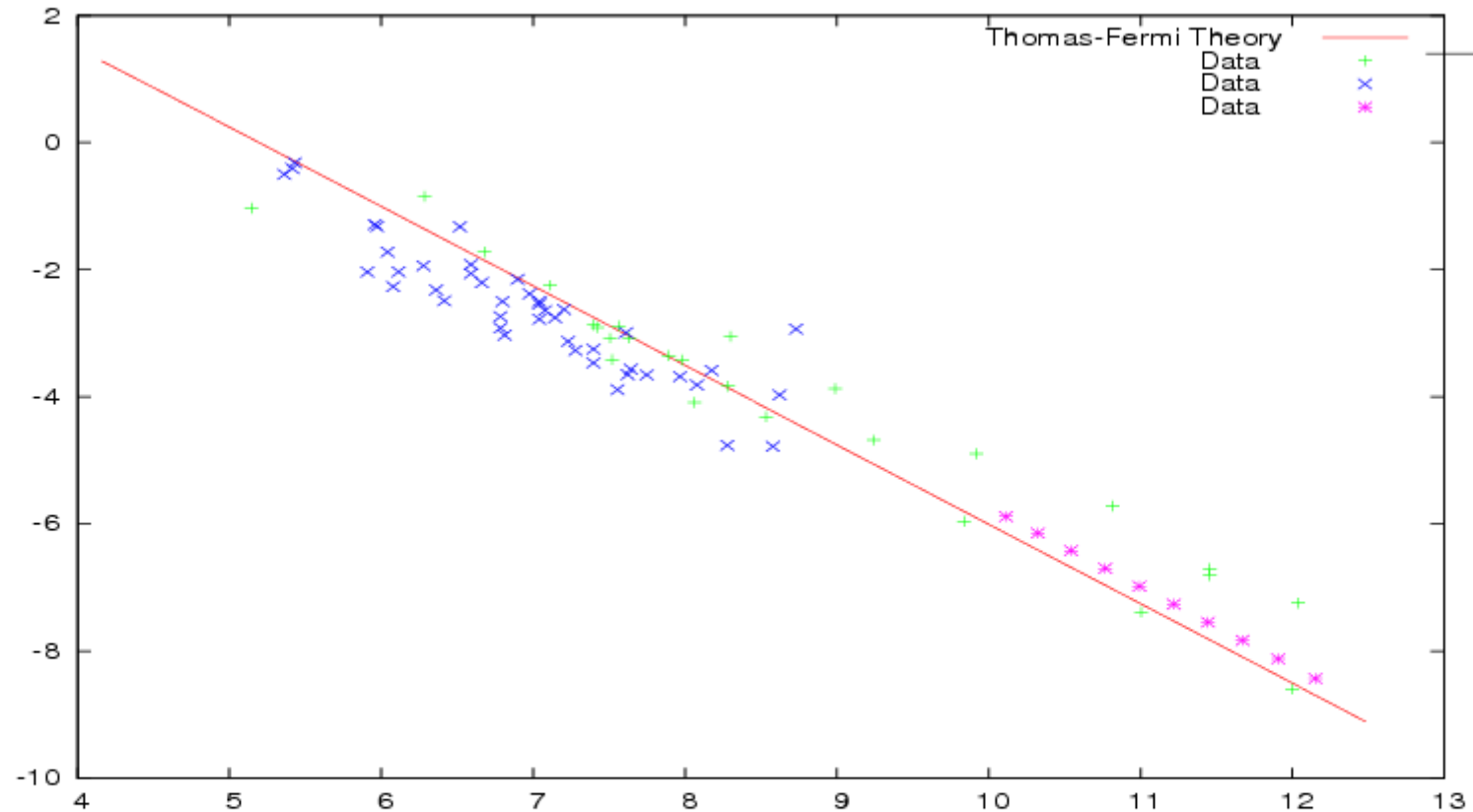
The minimal known halo mass is for Willman I:

$M_{Willman\,I} = 3.9\ 10^4\ M_\odot$ which implies $m \geq 1.86\ \mathrm{keV}$

Galaxy halo radius vs. Galaxy halo Mass
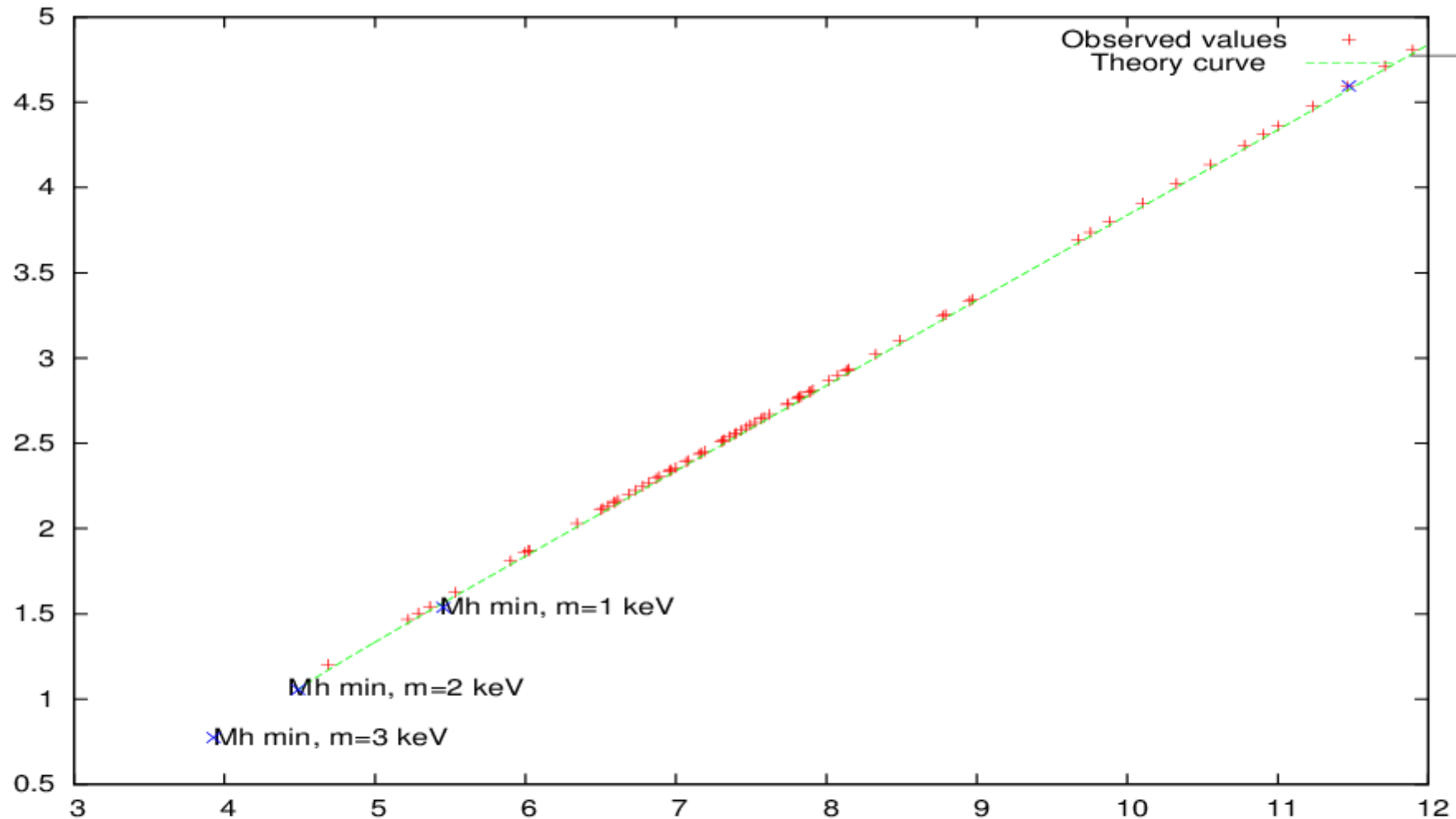
$\hat{r}_h = r_h \left(\Sigma_0 \, \mathrm{pc}^2 / [120 \, M_\odot]\right)^{\frac{1}{5}}$ vs. $\hat{M}_h = M_h \left(120 \, M_\odot / [\Sigma_0 \, \mathrm{pc}^2]\right)^{\frac{3}{5}}$.
r_h follows with precision the square-root of M_h and the amplitude factor as predicted theoretically.

Galaxy Phase-space density Q vs. Galaxy halo Mass

$\log_{10} Q$ vs. $\log_{10} \hat{M}_h$ theory and data.

$Q \equiv \rho(0)/\sigma^3(0)$. Theoretical curve Q obtained from the Thomas-Fermi expression.

Diluted regime of Galaxies

In the diluted regime of Galaxies

$$M_h \gtrsim 10^6 \, M_\odot \; , \quad \nu_0 \lesssim -5 \; , \quad T_0 \gtrsim 0.017 \text{ K} = 17 \text{ mK}.$$

r_h, M_h and $Q(0)$ scale as functions of each other.

$$M_h = 1.75572 \, \Sigma_0 \, r_h^2 \quad , \quad r_h = 68.894 \, \sqrt{\frac{M_h}{10^6 \, M_\odot}} \, \sqrt{\frac{120 \, M_\odot}{\Sigma_0 \, \text{pc}^2}} \; \text{pc}$$

$$Q(0) = 1.2319 \, \left(\frac{10^5 \, M_\odot}{M_h} \right)^{\frac{5}{4}} \, \left(\frac{\Sigma_0 \, \text{pc}^2}{120 \, M_\odot} \right)^{\frac{3}{4}} \; \text{keV}^4$$

These scaling behaviours are very accurate except near the degenerate limit.

C. Destri, H. J. de Vega, N. G. Sanchez, New Astronomy **22**, 39 (2013) and Astroparticle Physics, **46**, 14 (2013).
H. J. de Vega, P. Salucci, N. G. Sanchez, arXiv:1309.2290, to appear in MNRAS.
H. J. de Vega, N. G. Sanchez, arXiv:1310.6355.

Classical and Quantum regimes of WDM Galaxies

I. Diluted and classical regime:

$$\hat{M}_h \gtrsim 10^6 \; M_\odot \; , \quad \nu_0 \lesssim -5 \; , \quad T_0 \gtrsim 0.017 \; \text{K}.$$

The density and the velocity profiles are universal.

Exact scaling laws for r_h, M_h and $Q(0)$.

II. Quantum compact regime:

$$10^6 \; M_\odot \gtrsim \hat{M}_h \gtrsim \hat{M}_{h,min} = 3.1 \; 10^4 M_\odot \; ,$$

$$\nu_0 \gtrsim -5 \; , \quad 0 \leq T_0 \lesssim 0.017 \; \text{K}.$$

The density and the velocity profiles are non-universal: the profiles depend on the galaxy mass M_h.

Small deviations from the scaling laws for r_h, M_h and $Q(0)$.

III. Degenerate limit

$$\hat{M}_h = \hat{M}_{h,min} = 3.1 \; 10^4 \; M_\odot \; , \quad \nu_0 = +\infty \; , \quad T_0 = 0$$

Circular Velocities and Density Profiles

The circular velocity $v_c(r)$ follows from the virial theorem

$$v_c(r) = \sqrt{\frac{G\ M(r)}{r}} = \sqrt{-\frac{r}{m}\ \frac{d\mu}{dr}}$$

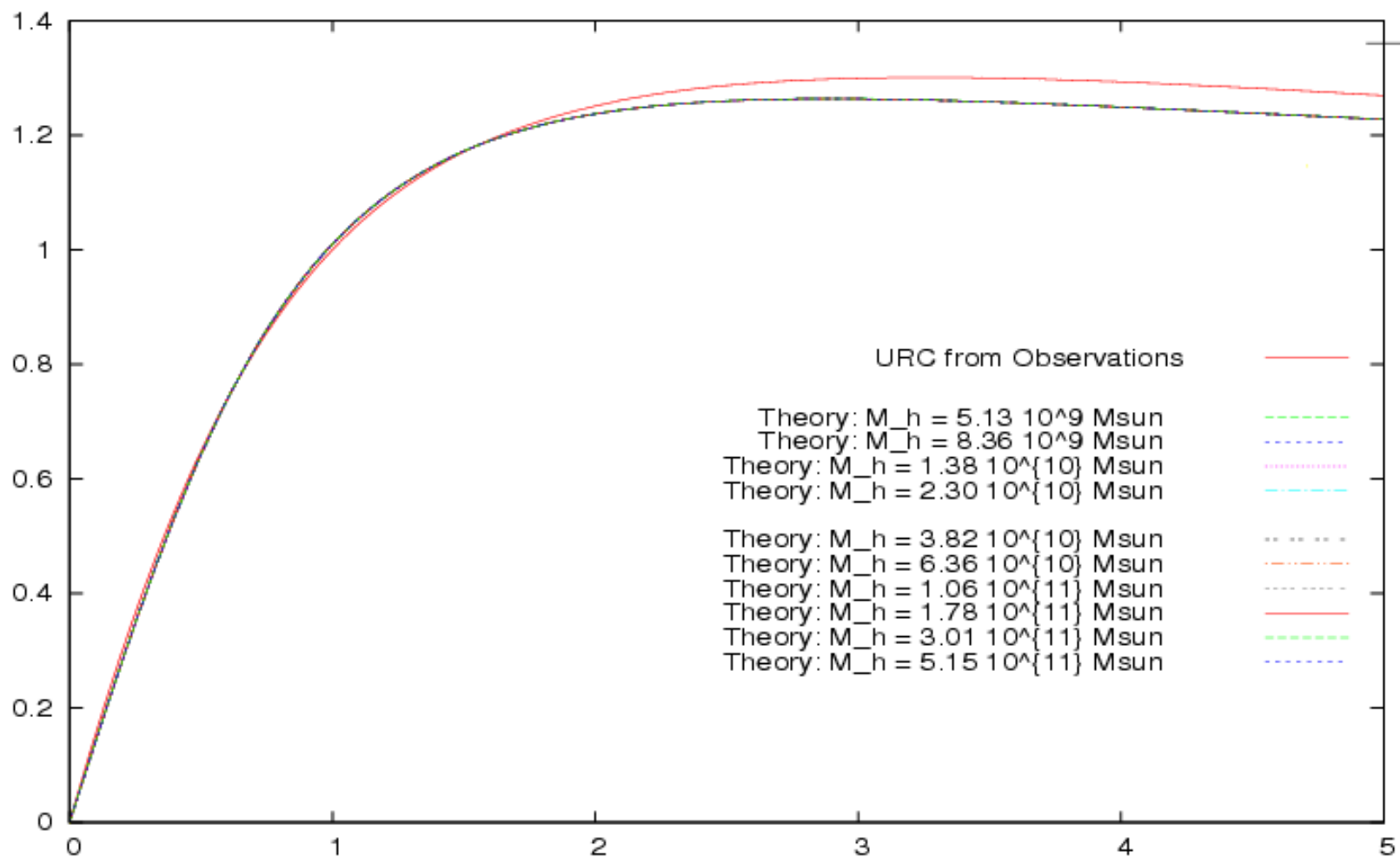The circular velocity normalized at the core radius r_h

$$U(x) \equiv \frac{v_c(r)}{v_c(r_h)} \quad , \quad x = \frac{r}{r_h}$$

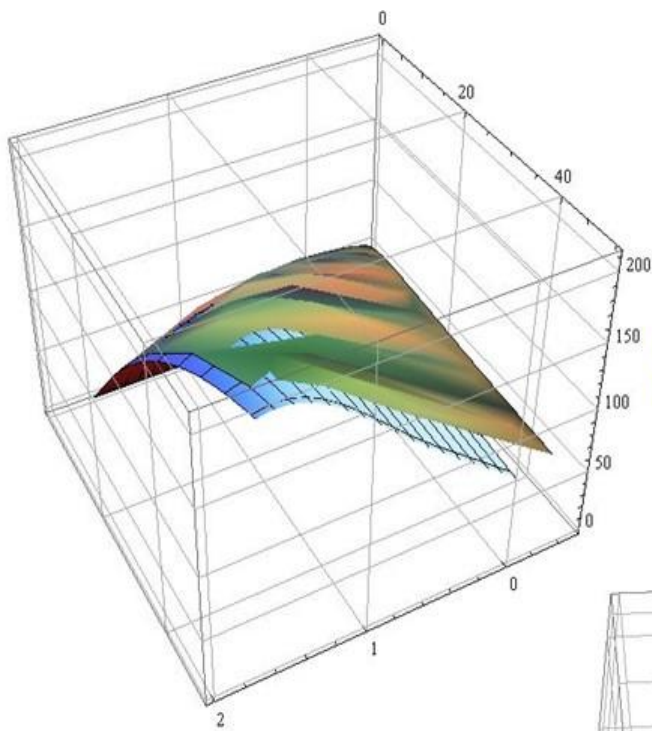Solving the Thomas-Fermi equations we find:

- $U(x) = v_c(r)/v_c(r_h)$ is only function of $x = r/r_h$.

- $U(x)$ takes the same values for all galaxy halo masses in the range $5.1\ 10^9\ M_\odot$ till $5.1\ 10^{11}\ M_\odot$.

- $U(x)$ turns to be an universal function.

- The observational universal curves and the theoretical Thomas-Fermi curves coincide for $r \lesssim 2\ r_h$, $x \lesssim 2$.
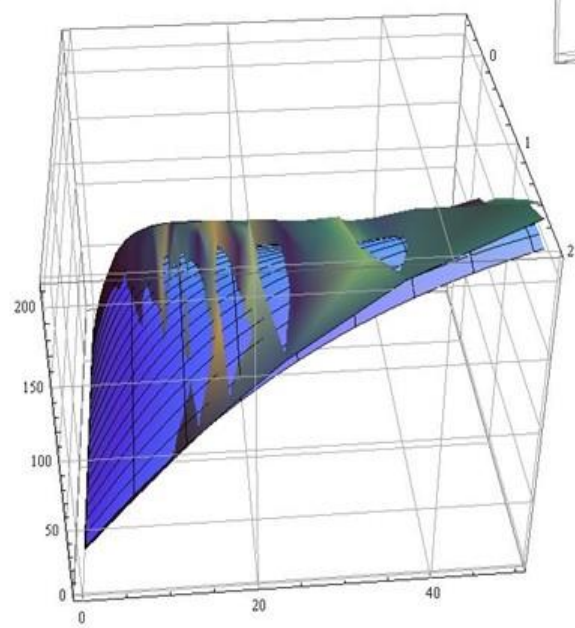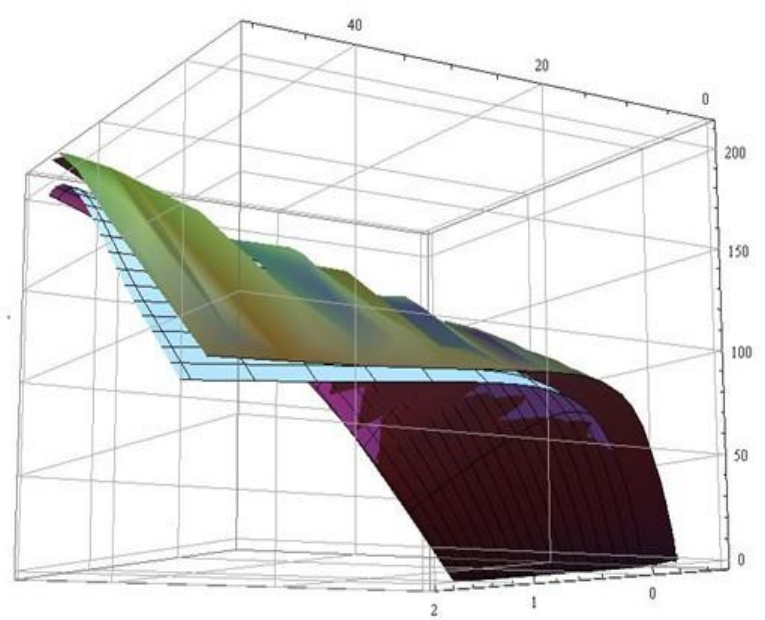
These are remarkable results !!

Normalized circular velocities

URC from Observations

Theory: M_h = 5.13 10^9 Msun
Theory: M_h = 8.36 10^9 Msun
Theory: M_h = 1.38 10^{10} Msun
Theory: M_h = 2.30 10^{10} Msun

Theory: M_h = 3.82 10^{10} Msun
Theory: M_h = 6.36 10^{10} Msun
Theory: M_h = 1.06 10^{11} Msun
Theory: M_h = 1.78 10^{11} Msun
Theory: M_h = 3.01 10^{11} Msun
Theory: M_h = 5.15 10^{11} Msun

$$U(x) = v_c(r)/v_c(r_h) \quad \textbf{vs.} \quad x = r/r_h.$$
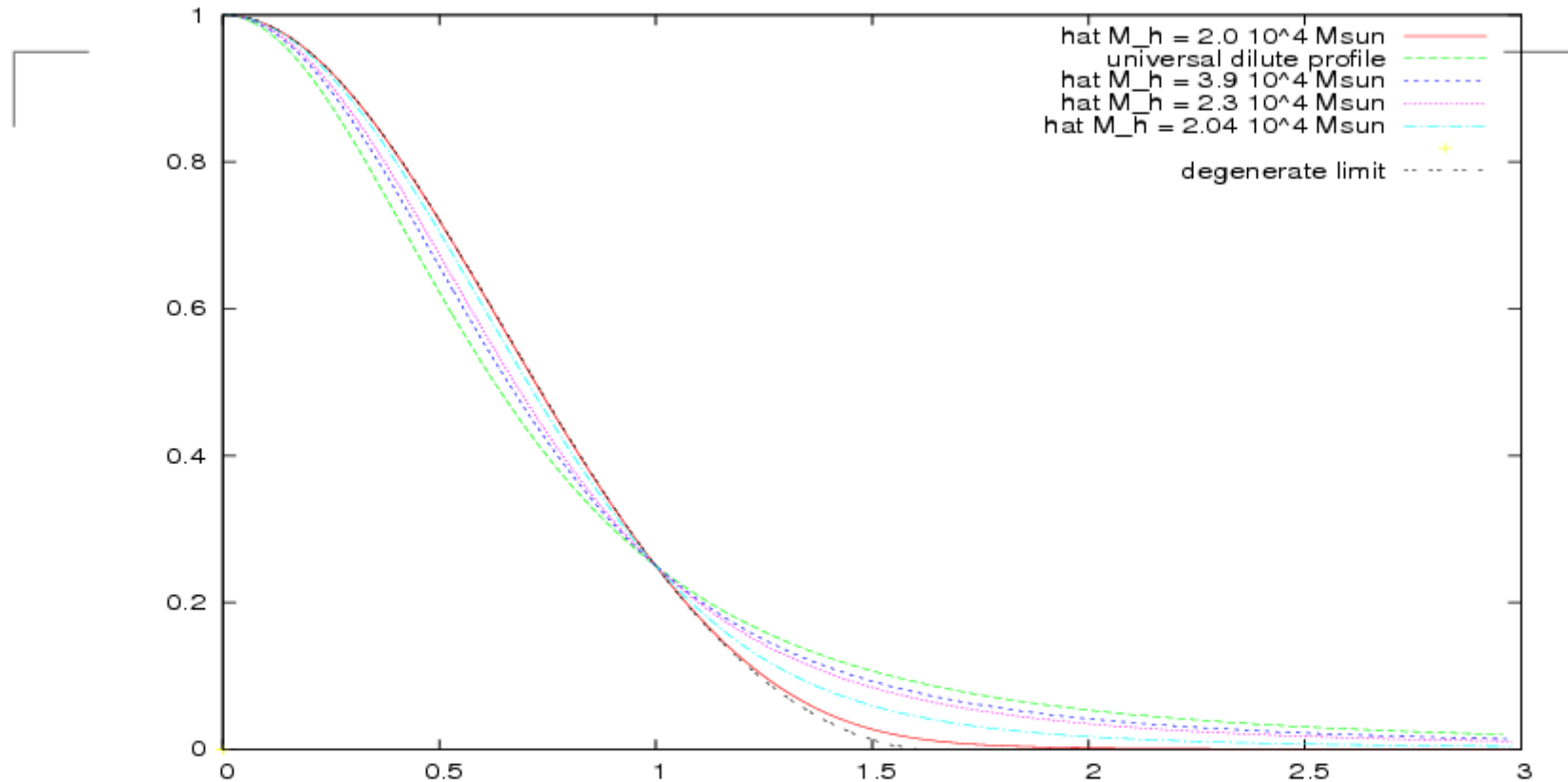
2 keV th
2-10 keV X

Theoretical vs. observational density profiles
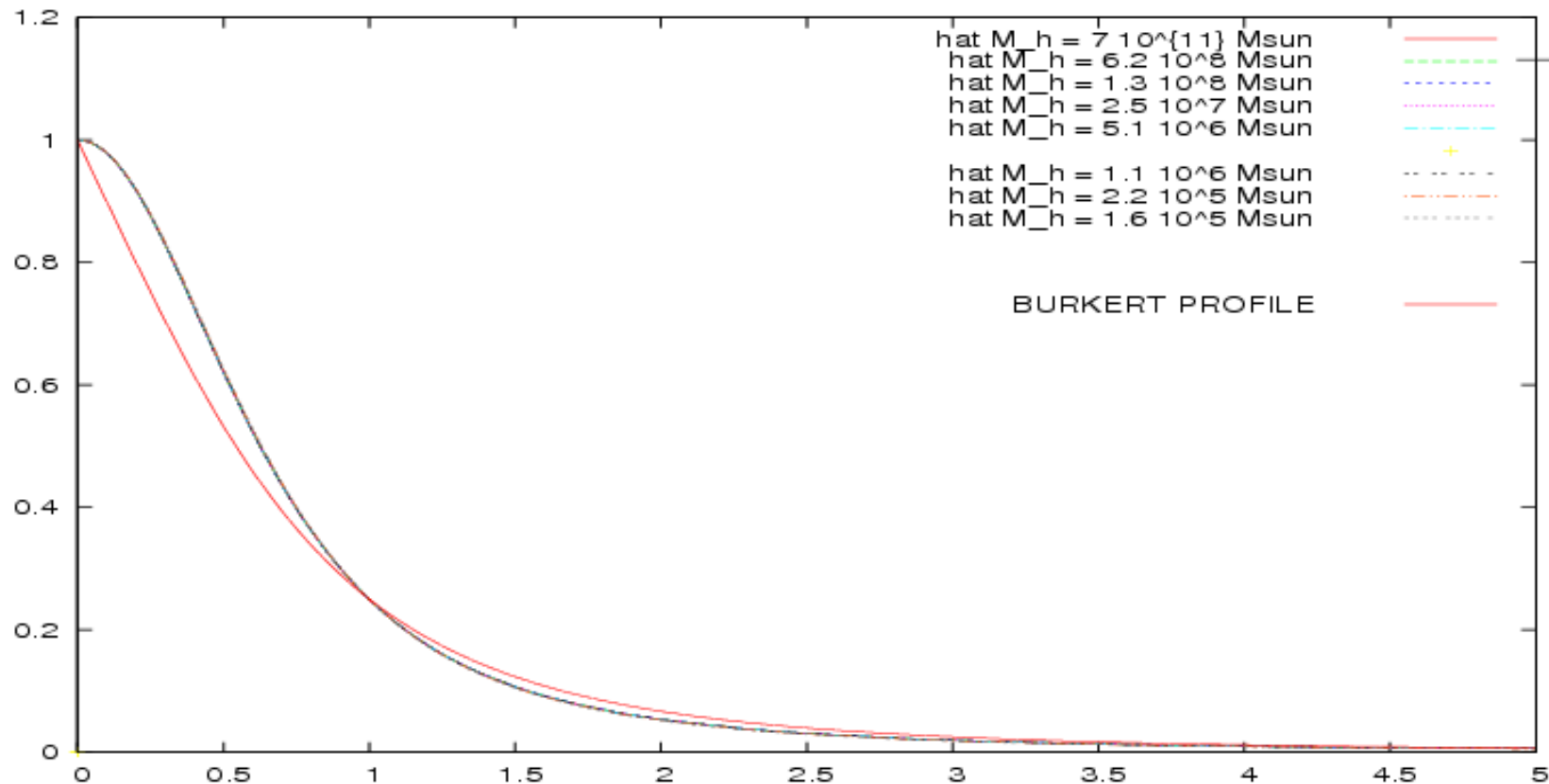
$\rho(r)/\rho(0)$ as functions of r/r_h. **ALL** the theoretical profiles in the diluted regime: $1.4\ 10^5\ M_\odot < \hat{M}_h < 7.5\ 10^{11}\ M_\odot$ **fall** into the same and universal density profile in very good agreement with the empirical Burkert profile.

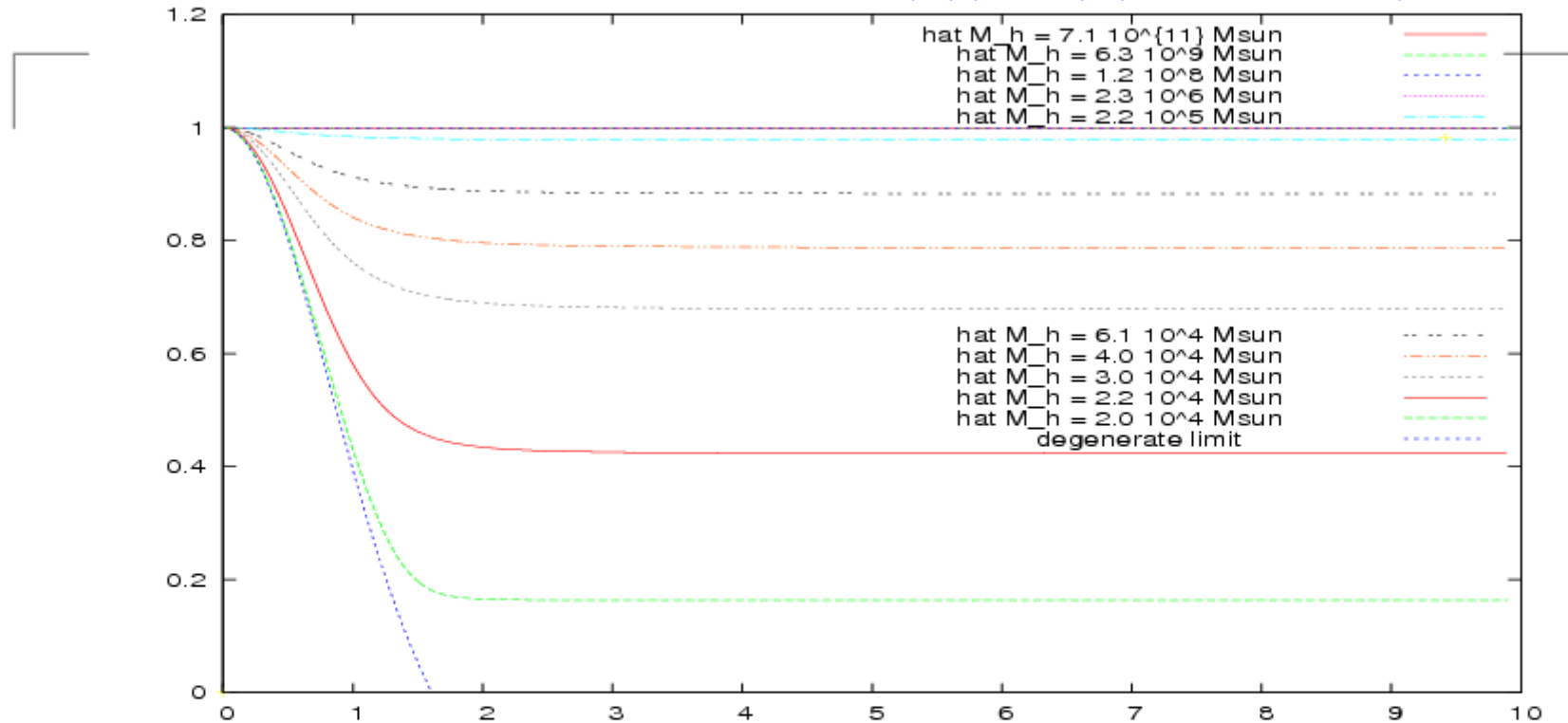# Density profiles in the Quantum regime

$\rho(r)/\rho(0)$ as functions of r/r_h.

Galaxy halo masses $M_h^{min} = 3.1\ 10^4\ M_\odot \leq \hat{M}_h < 3.9\ 10^4\ M_\odot$ in the quantum regime exhibit shrinking density profiles.

Velocity dispersion profiles $\sigma^2(r)/\sigma^2(0)$ vs. $x = r/r_h$

ALL velocity profiles in the classical diluted regime
$\hat{M}_h > 2.3\ 10^6\ M_\odot$ fall into a constant universal value.
In the quantum regime: $1.6\ 10^6 M_\odot > \hat{M}_h > \hat{M}_{h,min}$ the
profiles are not universal and do depend on $\hat{M}_h$ and x.

The local equation of state of WDM Galaxies

The pressure $P(r)$ as a function of the density $\rho(r)$

$$\rho = \frac{m^{\frac{5}{2}}}{3\,\pi^2\,\hbar^3}\,(2\,T_0)^{\frac{3}{2}}\,I_2(\nu) \quad , \quad P = \frac{m^{\frac{3}{2}}}{15\,\pi^2\,\hbar^3}\,(2\,T_0)^{\frac{5}{2}}\,I_4(\nu).$$

through the parameter ν from the Thomas-Fermi equation.

$$P = \frac{T_0}{m}\,\rho \quad , \quad \nu \ll -1, \text{ WDM diluted galaxies.}$$

$$P = \frac{\hbar^2}{5}\,\left(\frac{3\,\pi^2}{m^4}\right)^{\frac{2}{3}}\,\rho^{\frac{5}{3}} \; , \; \nu \gg 1, \text{ WDM degenerate quantum limit.}$$

Simple formula accurately representing the exact equation of state obtained by solving the Thomas-Fermi equation:
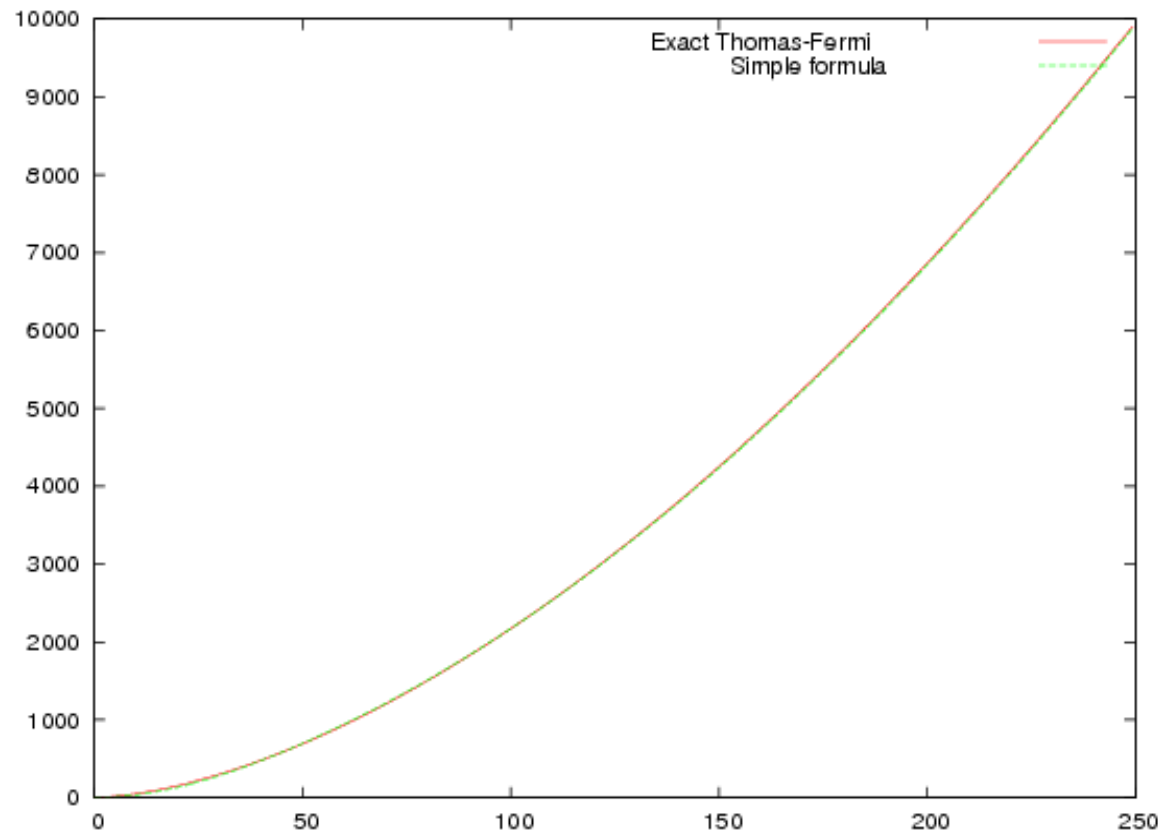
$$P = \frac{m^{\frac{3}{2}}\,(2\,T_0)^{\frac{5}{2}}}{15\,\pi^2\,\hbar^3}\,\left(1 + \frac{3}{2}\,e^{-\beta_1\,\tilde{\rho}}\right)\,\tilde{\rho}^{\frac{1}{3}\left(5 - 2\,e^{-\beta_2\,\tilde{\rho}}\right)},$$

$$\tilde{\rho} \equiv \frac{3\,\pi^2\,\hbar^3}{m^{\frac{5}{2}}\,(2\,T_0)^{\frac{3}{2}}}\,\rho = I_2(\nu),$$

best fit to the Thomas-Fermi equation of state for:

$$\beta_1 = 0.047098 \quad , \quad \beta_2 = 0.064492$$

The equation of state of Galaxies: exact T-F and simple formula

The equation of state $\tilde{P}$ vs. $\tilde{\rho}$ obtained by solving the Thomas-Fermi equation and the simple formula.

$$\tilde{P} = \frac{15\,\pi^2\,\hbar^3}{m^{\frac{3}{2}}\,(2\,T_0)^{\frac{5}{2}}}\,P = I_4(\nu)\ ,\quad \tilde{\rho} \equiv \frac{3\,\pi^2\,\hbar^3}{m^{\frac{5}{2}}\,(2\,T_0)^{\frac{3}{2}}}\,\rho = I_2(\nu)$$

The Eddington equation for Dark Matter in Galaxies

$f(E)$ DM distribution function, $E = p^2/(2m) - \mu$,
m DM particle mass, μ the chemical potential.

Equilibrium condition: $\mu(r) = \mu_0 - m\,\phi(r)$,

$\phi(r) =$ gravitational potential.

The Poisson equation takes the self-consistent form:

$$\frac{d^2\mu}{dr^2} + \frac{2}{r}\frac{d\mu}{dr} = -4\pi G m\,\rho(r) = -\frac{4\,G\,m^2}{\pi\,\hbar^3}\int_0^\infty dp\,p^2 f\left[\frac{p^2}{2m} - \mu(r)\right]$$

Dimensionless variables: q, $\nu(q)$:

$$r = r_h\,q \quad,\quad \mu(r) = T_0\,\nu(q) \quad,\quad f(E) = \Psi(E/T_0)$$

T_0 plays the role of the temperature and depends on the galaxy mass. The density profile is known from the observations:

$$\rho(r) = \rho_0\,F\left(\frac{r}{r_h}\right) = \rho_0\,F(q)\;,\;\rho_0 \equiv \rho(0)\;,\;F(1) = 1/4.$$

To be determined: the DM distribution function $\Psi(E/T_0)$.

Abel's equation and its solution

Dimensionless Poisson's equation:

$$\frac{d^2\nu}{dq^2} + \frac{2}{q}\frac{d\nu}{dq} = -b_0\, F(q)\ ,\ b_0 \equiv 4\,\pi\,G\,\rho_0\,r_h^2\,\frac{m}{T_0}$$

$$\nu(q) = \nu(0) + b_0\,\varepsilon(q)\ ,\ \varepsilon(q) - \int_0^q \left(1 - \frac{q'}{q}\right) q'\, F(q')\, dq'$$

Self-consistent Poisson equation in dimensionless variables:

$$\rho(r) = \frac{\sqrt{2}}{\pi^2}\, m^{\frac{5}{2}}\, T_0^{\frac{3}{2}} \int_{\nu(\infty)}^{\nu} d\nu'\, \sqrt{\nu - \nu'}\ \Psi(-\nu')\ ,\ \nu' \equiv \nu - \frac{p^2}{2\,m\,T_0}.$$

and in terms of the density profile $F(q)$

$$F(\nu) = \frac{\sqrt{2}}{\pi^2}\, \frac{m^{\frac{5}{2}}\, T_0^{\frac{3}{2}}}{\rho_0}\, \int_{\nu(\infty)}^{\nu} d\nu'\, \sqrt{\nu - \nu'}\ \Psi(-\nu')$$

This is an **Abel integral** equation and its solution, the **Eddington formula**:

$$\Psi(-\nu) = \sqrt{2}\,\pi\, \frac{\rho_0}{m^{\frac{5}{2}}\, T_0^{\frac{3}{2}}}\, \int_{\nu(\infty)}^{\nu} \frac{d\nu'}{\sqrt{\nu - \nu'}}\, \frac{d^2 F}{d\nu'^2}$$

Boundary condition: Ψ and $d\Psi/d\nu$ vanish at infinite distance.

The Halo Dark Matter equation of state from the density profile

From the density profile we obtained the pressure and therefore the DM equation of state

$$\frac{P(r)}{\rho(r)} = \frac{1}{3}\, v^2(r) = G\,\Sigma_0\, r_h\, \frac{\Pi(q)}{F(q)}$$

The local temperature $T(r)$ is given by $T(r) = \frac{1}{3}\, m\, v^2(r)$.

Hence, the dark matter obeys locally an ideal gas equation of state

$$P(r) = \frac{T(r)}{m}\, \rho(r)\ , \ T(r) \equiv m\, G\, \Sigma_0\, r_h\, t(q)\ , \ t(q) \equiv \frac{\Pi(q)}{F(q)}$$

The temperature $T(r)$ turns to be approximately constant inside the halo radius $r \lesssim r_h\ : t(q) \simeq 1.419$.

$$T(r) = 8.238\, t(q)\, \frac{m}{2\,\text{keV}}\, \sqrt{\frac{\Sigma_0\,\text{pc}^2}{120\, M_\odot}\, \frac{M_h}{10^6\, M_\odot}}\ \text{mK}$$

The temperature grows as the square root of the galaxy halo mass.

The Distribution Function in terms of the Density Profile

We explicitly find the distribution function $\Psi(q)$ in terms of the density profile $F(q)$ in H. J. de Vega, N. G. Sanchez, arXiv:1401.0726.

$$\Psi(q) = \frac{1}{G^{\frac{3}{2}} \, r_h^3 \, m^4 \, \sqrt{\rho_0}} \, \mathcal{D}(q) \,, \; \mathcal{D}(q) \equiv \frac{1}{\sqrt{32}\,\pi} \int_q^\infty \frac{\mathcal{J}(q')\,dq'}{\sqrt{\varepsilon(q)-\varepsilon(q')}}$$

$$\mathcal{J}(q) \equiv \frac{1}{\left(-\dfrac{d\varepsilon}{dq}\right)} \left[\frac{d^2 F}{dq^2} - \frac{\dfrac{d^2\varepsilon}{dq^2}}{\dfrac{d\varepsilon}{dq}} \, \frac{dF}{dq} \right]. \text{ Notice that } \left(-\frac{d\varepsilon}{dq} > 0 \right).$$

We explicitly find the velocity dispersion and the pressure in terms of the density profile $F(q)$:

$$v^2(r) = 6\,\pi\,G\,\rho_0\,r_h^2\,\frac{1}{F(q)} \int_q^\infty dq' \, [\varepsilon(q) - \varepsilon(q')]^2 \; \mathcal{J}(q')$$

$$P(r) = 2\,\pi\,G\,\Sigma_0^2 \int_q^\infty dq' \, [\varepsilon(q) - \varepsilon(q')]^2 \; \mathcal{J}(q')$$

Physical results from the Distribution Function

Cored density profiles behaving quadratically for small distances $\rho(r) \stackrel{r \Rightarrow 0}{=} \rho(0) - K\, r^2$ produce finite and positive distribution functions at the halo center while cusped density profiles always produce divergent distribution functions at the center.

We explicitly compute the phase–space distribution function and the equation of state for the family of α-density profiles

$$\rho(r) = \frac{\rho_0}{\left[1 + \left(\dfrac{r}{r_h} \right)^2 \right]^\alpha} \quad , \quad 1 \le \alpha \le 2.5$$

This cored density profile generalizes the pseudo-thermal profile and with $\alpha \sim 1.5$, it is perfectly appropriate to fit galaxy observations.

For $\alpha = 5/2$ this is the Plummer profile describing the density of stars in globular clusters.

Halo Thermalization from the Distribution Function

The obtained distribution function $\Psi(q)$ is **positive** for all values of q in the whole range $1 \leq \alpha \leq 2.5$. Therefore, the α−profiles are physically meaningful. [In general, there is no guarantee that $\Psi(q)$ from the Eddington formula will be nowhere negative.]

$\ln \mathcal{D}(-\varepsilon)$ is approximately a linear function of the energy $-\varepsilon$ for $\alpha \sim 1.5$ and $0 < -\varepsilon \lesssim 0.6$ which corresponds to $0 < r \lesssim 7\, r_h$.

Therefore, the distribution function corresponding to α−profiles for $\alpha \sim 1.5$ is approximately a thermal Boltzman distribution in this interval. These are realistic halo galaxy density profiles.

The galaxy halos are therefore thermalized, supporting and confirming the Thomas-Fermi WDM approach.

Halo Thermalization
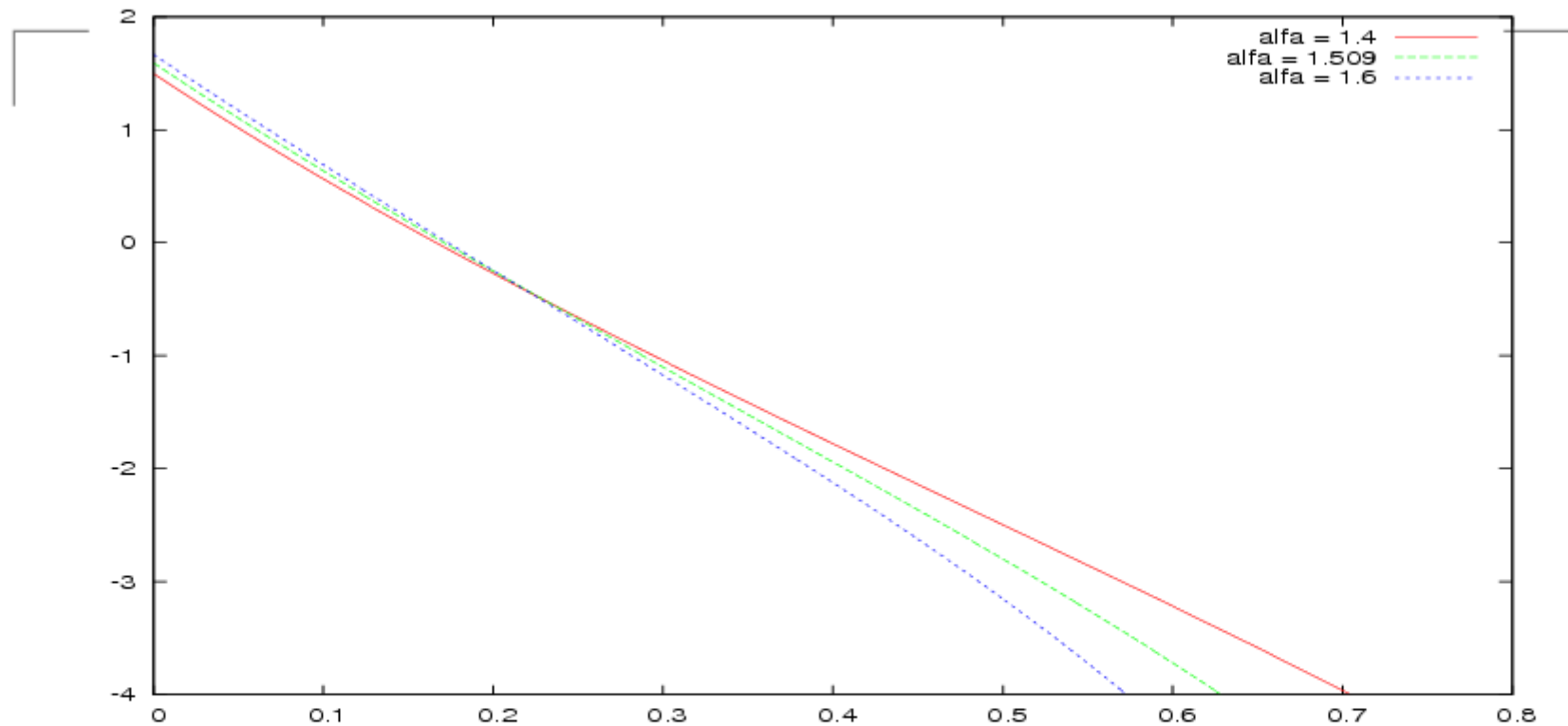
The distribution function $\ln \mathcal{D}(-\varepsilon)$ vs. the energy $-\varepsilon$.

This linear behaviour of $\ln \mathcal{D}(-\varepsilon)$ indicates a Boltzman distribution function for $0 \leq -\varepsilon \lesssim 0.7$ and $0 < r \lesssim 7\, r_h$. No assumption about the DM particle nature is made here.

Circular velocity and circular temperature

The circular velocity and the circular temperature are defined by the virial theorem:

$$v_c^2(r) \equiv \frac{G\,M(r)}{r} \; , \; T_c(r) \equiv \frac{1}{3}\,m\,v_c^2(r) = \frac{G\,m\,M(r)}{3\,r}$$

$$T_c(r) = m\,G\,\rho_0\,r_h^2\,t_c(q)$$
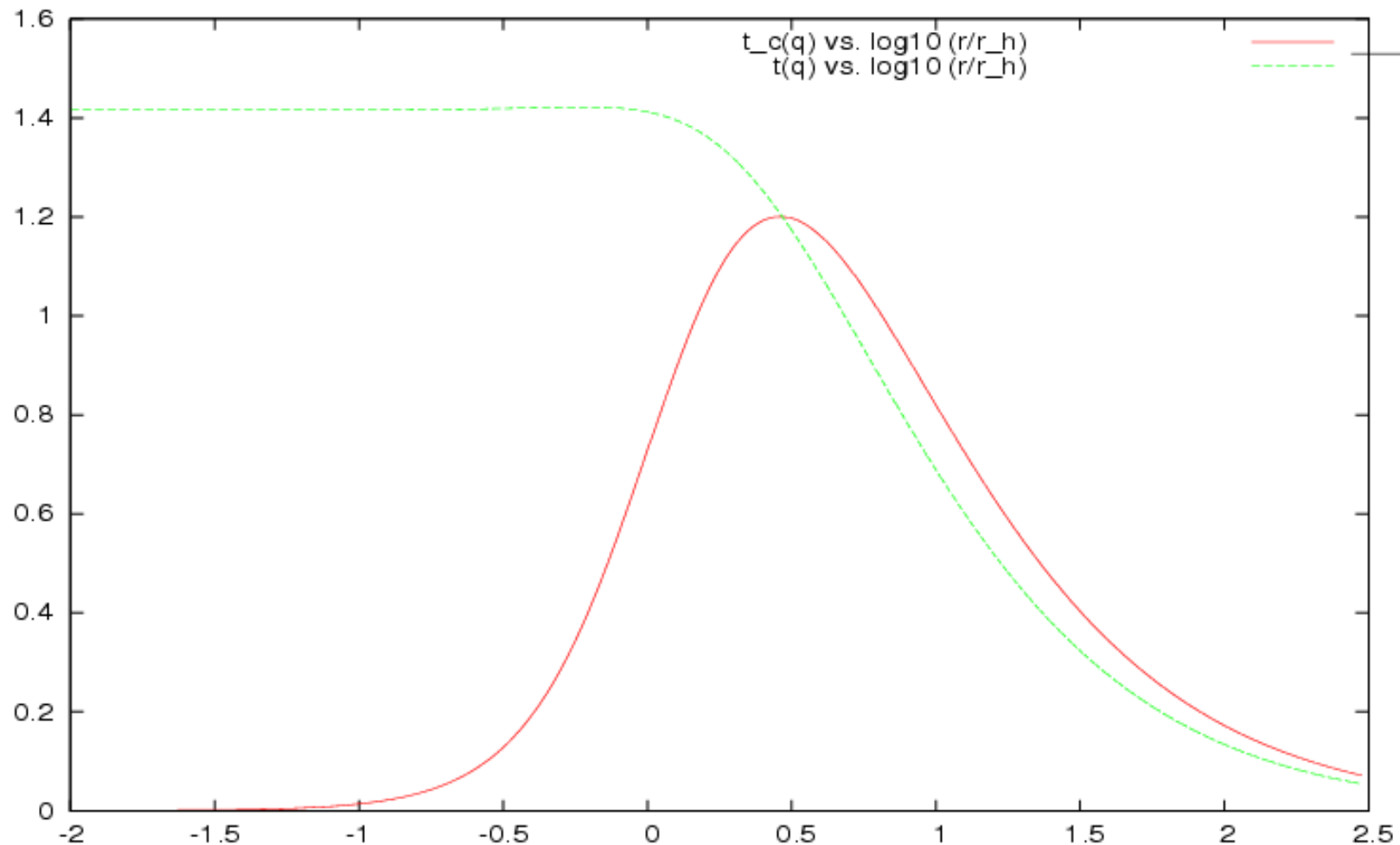
The local temperature $t(q)$ turns to follow the decrease of the circular temperature $t_c(q)$ for $r \gtrsim r_h$.

Conclusion:

- Halo thermalization for $r < r_h$.
- Halo virialization for $r > r_h$.

H. J. de Vega, N. G. Sanchez, arXiv:1401.0726

Thermalization and Virialization

The normalized temperature $t(r/r_h)$ and the circular temperature $t_c(r/r_h)$ vs. $\log_{10}(r/r_h)$ for $\alpha = 1.509$.

For $r \gtrsim r_h$, the local temperature decreases slowly with r.

THE MINIMAL GALAXY MASS

A minimal galaxy mass and minimal velocity dispersion are found.

This in turn implies a **minimal mass m_min** =1.91 keV for the WDM particle.

This **minimal WDM mass** is a **universal** value, independent of the WDM particle physics model because only relies on the **degenerate quantum fermion state**, which is universal whatever is the non-degenerate regime.

These results and the observed halo radius and mass of the compact galaxies also **provide further indication that the WDM particle mass m is approximately around 2 keV.**

More precise data will make this estimation more precise.

Minimal galaxy mass from degenerate WDM

The halo radius, the velocity dispersion and the galaxy mass take their minimum values for degenerate WDM:

$$r_{h\ min} = 24.51\ldots \text{ pc } \left(\frac{m}{\text{keV}}\right)^{\frac{4}{3}} \left[\rho(0)\frac{\text{pc}^3}{M_\odot}\right]^{\frac{1}{6}}$$

$$M_{min} = 2.939\ldots 10^5\ M_\odot \left(\frac{\text{keV}}{m}\right)^4 \sqrt{\rho(0)\frac{\text{pc}^3}{M_\odot}}$$

$$\sigma_{min}(0) = 2.751\ldots \frac{\text{km}}{\text{s}}\ \left(\frac{\text{keV}}{m}\right)^{\frac{4}{3}} \left[\rho(0)\frac{\text{pc}^3}{M_\odot}\right]^{\frac{1}{3}}.$$

These minimum values correspond to the observations of compact dwarf galaxies.

Lightest known compact dwarf galaxy is Willman I:
$$M_{Willman\ I} = 2.9\ 10^4\ M_\odot$$

Imposing $M_{Willman\ I} > M_{min}$ yields the lower bound for the WDM particle mass: $m > 1.91$ keV.

WARM DARK MATTER REPRODUCE

→OBSERVED GALAXY DENSITIES
AND VELOCITY DISPERSIONS

→OBSERVED GALAXY
CORED DENSITY PROFILES

->OBSERVED SURFACE DENSITY VALUES OF
DARK MATTER DOMINATED GALAXIES

→SOLVES the OVERABUNDANCE (õsatellite)
PROBLEM and the CUSPS vs CORES Problem

Summary Warm Dark Matter, WDM: $m \sim$ keV

- Large Scales, structures beyond ~ 100 kpc: WDM and CDM yield identical results which agree with observations

- Intermediate Scales: WDM give the correct abundance of substructures.

- Inside galaxy cores, below ~ 100 pc: N-body classical physics simulations are incorrect for WDM because of important quantum effects.

- Quantum calculations (Thomas-Fermi) give galaxy cores, galaxy masses, velocity dispersions and densities in agreement with the observations.

- Direct Detection of the main WDM candidate: the sterile neutrino. Beta decay and electron capture. ^{3}H, Re, Ho.

So far, not a single valid objection arose against WDM.

Baryons (=16%DM) expected to give a correction to WDM

É WDM OVERALL CONCLUSION

É **To conclude, we find it is highly remarkable that in the context of warm dark matter, the quantum description provided by this semiclassical framework, (quantum WDM and classical gravitation), is able to reproduce such broad variety of galaxies.**

É **The resulting galaxy, halo radius, galaxy masses and velocity dispersion are fully consistent with observations for all different types of galaxies. Fermionic WDM treated quantum mechanically, as it must be, is able to reproduce the observed galactic cores and their sizes. In addition, WDM simulations produce the right DM structures in agreement with observations for scales > kpc.**

WDM + BARYONS

Baryons have not been included in this study. This is fully justified because on one hand **dwarf compact galaxies are composed today 99.99 % of DM, and** on the other hand **the baryon fraction in large galaxies can reach values up to 1 - 3 %.**

Since Fermionic WDM by itself produces galaxies and structures in agreement with observations for all types of galaxies, masses and sizes, the effect of including baryons is expected to be a small correction to these pure WDM results, consistent with the fact that dark matter is in average six times more abundant than baryons.

Axions are ruled out as dark matter

Hot Dark Matter (eV particles or lighter) are ruled out because their free streaming length is too large $\gtrsim$ Mpc and hence galaxies are not formed.

A Bose-Einstein condensate of light scalar particles evades this argument because of the quantum nature of the BE condensate. $r_{Jeans} \sim 5$ kpc implies $m_{axion} \sim 10^{-22}$ eV.

The phase-space density $Q = \rho/\sigma^3$ decreases during structure formation: $Q_{today} < Q_{primordial} \propto m^4$.

Computing $Q_{primordial}$ for a DM BE condensate we derived lower bounds on the DM particle mass m using the data for Q_{today} in dwarf galaxies:

TE: $m \geq 0.155$ MeV $\left(\frac{25}{g_d}\right)^{5/3}$. Out of TE: $m \geq 14$ eV $\left(\frac{25}{g_d}\right)^{5/3}$

Axions with $m \sim 10^{-22}$ eV are ruled out as DM candidates.

D. Boyanovsky, H. J. de Vega, N. G. Sanchez, PRD 77, 043518 (08). H. de Vega, N. Sanchez, arXiv:1401.1214

X-ray detection of DM sterile neutrinos

Sterile neutrinos ν_s decay into active neutrinos ν_e plus X-rays with a lifetime $\sim 10^{11} \times$ age of the universe.

These X-rays may be seen in the sky looking to galaxies ! recent review: C. R. Watson et al. JCAP, (2012).

Future observations:

- Satellite projects: Xenia (NASA), ASTRO-H (Japan).

- CMB: WDM decay distorts the blackbody CMB spectrum. The projected PIXIE satellite mission (A. Kogut et al.) can measure WDM sterile neutrino mass.

- PTOLEMY experiment: Princeton Tritium Observatory. Aims to detect the cosmic neutrino background and WDM (keV scale) sterile neutrinos through the electron spectrum of the Tritium beta decay induced by the capture of a cosmic neutrino or a WDM sterile neutrino.

- HOLMES electron capture in ^{163}Ho calorimeter G Sasso

Summary and Conclusions

- Combining theoretical evolution of fluctuations through the Boltzmann-Vlasov equation with galaxy data points to a DM particle mass 3 - 10 keV. T_d turns to be model dependent. The keV mass scale holds independently of the DM particle physics model.

- Universal Surface density in DM galaxies $[\mu_{0D} \simeq (18 \text{ MeV})^3]$ explained by keV mass scale DM. Density profile scales and decreases for intermediate scales with the spectral index n_s : $\rho(r) \sim r^{-1-n_s/2}$ and $\rho(r) \sim r^{-2}$ for $r \gg r_0$.

H. J. de Vega, P. Salucci, N. G. Sanchez, 'The mass of the dark matter particle from theory and observations', New Astronomy, 17, 653 (2012).

H. J. de Vega, N. Sanchez, 'Model independent analysis of dark matter points to a particle mass at the keV scale', MNRAS 404, 885 (2010)

Future Perspectives: Detection!

Sterile neutrino detection depends upon the particle physics model. There are sterile neutrino models where the keV sterile is stable and thus hard to detect.

Astronomical observation of steriles:
X-ray data from galaxy halos.

Direct detection of steriles in Lab:

Bounds on mixing angles from
Mare, Katrin, ECHo, Project 8 and PTOLEMY are expected.

For a particle detection a dedicated beta decay or electron capture experiment looks necessary to search sterile neutrinos with mass around 2 keV.

Calorimetric techniques seem well suited.

Best nuclei for study:

Electron capture in ^{163}Ho, beta decay in ^{187}Re and Tritium.

Future Perspectives: Detection!

Sterile neutrino detection depends upon the particle physics model. There are sterile neutrino models where the keV sterile is stable and thus hard to detect.

Astronomical observation of steriles: X-ray data from galaxy clusters (Bulbul et al. 2014) and galaxy halos.

Direct detection of steriles in Lab:

Bounds on mixing angles from
Mare, Katrin, ECHo, Project 8 and PTOLEMY are expected.

For a particle detection a dedicated beta decay or electron capture experiment looks necessary to search sterile neutrinos with mass in the keV scale.

Calorimetric techniques seem well suited.

Best nuclei for study: Electron capture in ^{163}Ho, beta decay in ^{187}Re and Tritium.

2014 DARK MATTER UPDATE

É **THERE IS NO CUSP/CORE problem:**

É **Observed Galaxy profiles are cored.**

É **WDM Galaxy density profiles are cored**

É **THERE IS NO satellite problem**

É **WDM abundance of structures agrees with observations**

É In addition, these are not fundamental problems.

NO DM WIMPS, NO DM annhilation,

NO DM axions

END

THANK YOU FOR YOUR ATTENTION

UNDER COMPLETION NOW

H. J. de Vega, N. G. Sanchez:
BLACK HOLES FORMED
by WDM and BARYONS

(GALACTIC SUPERMASSIVE, STELLAR)

Stars, globular clusters, galaxies,Å . galaxy clusters
And other resultsÅ ..

École Internationale Daniel Chalonge

Science with great intellectual endeavour and a human face
La science qui donne envie. Une grande aventure scientifique et humaine

23 Years of Activity. Calling for understanding

PROGRAMME OF THE YEAR 2014

14 MARCH 2014: Opening Session / Session ouverte de culture scientifique : "Présentation du programme 2014 et des dernières nouvelles scientifiques de l'univers" *(Batiment Perrault, Observatoire de Paris)*

22 MAY 2014: Spring Open Session of scientific culture / Session ouverte de printemps de culture scientifique interdisciplinaire : "L'homme et l'univers" *(Bâtiment Perrault, Observatoire de Paris)*

4-7 JUNE 2014: Chalonge Meudon workshop: "From large to small scale structures in agreement with observations: CMB, WDM, galaxies, black holes, neutrinos and sterile neutrinos" *(Château de Meudon - CIAS, Meudon)*

22-25 JULY 2014: The 18th Paris cosmology colloquium Chalonge 2014: "Latest news from the universe: Λ WDM, CMB, dark matter, Λ dark energy, neutrinos and sterile neutrinos" *(Bâtiment Perrault, Observatoire de Paris)*

25 JULY 2014: Summer Open Session of scientific culture / Session ouverte d'Été de culture scientifique : A surprise session

AUTOMNE 2014: Cycle Les grandes questions posées aujourd'hui à la science : "Où va la science ?" *(Cité Internationale Universitaire de Paris)*

17-18 OCTOBER 2014: Chalonge Turin session: "Latest news from the universe: dark matter, galaxies and particle physics" *(Palazzo de l'Università & Accademia delle Scienze, Piamonte region, Turin, Italy)*

27-28 NOVEMBER 2014: Concluding session & Avant-première 2015

Welcome to the Chalonge School: A laboratory of ideas, Research, Training, Scientific Culture

A beacon pioneering and developing research, projects and training. The programme offers invaluable international current research view at the forefront of astrophysics and cosmology, international contacts at the highest level and a careful interdisciplinarity, with both theory and observations.

The programme is open to researchers, post-docs and advanced students of the different disciplines in the field, both theorists, experimentalists and observers. Advanced students, post-docs, young researchers are encouraged to participate. The programme includes scientific culture events with the latest results and exhibitions.

The Chalonge School Medal is coined exclusively for the Chalonge School by the *Hôtel de la Monnaie de Paris* (the French Mint). Only ten Chalonge medals have been awarded in the 22 year school history.

Awarded Daniel Chalonge Medals

Subramanyan CHANDRASEKHAR, *Nobel prize of physics*
Bruno PONTECORVO
George SMOOT, *Nobel prize of physics*
Carlos FRENK
Anthony LASENBY
Bernard SADOULET, *Fellow of the USA Academy of Arts And Sciences*
Peter BIERMANN
John MATHER, *Nobel prize of physics*
Brian SCHMIDT, *Nobel prize of Physics*
Gérad GILMORE, *Fellow of the UK Royal Society*

The Chalonge School Team

Science Organizers
Norma G. SANCHEZ, Héctor J. DE VEGA, Maria C. FALVELLA, Alba ZANINI, Marina RAMON MEDRANO, Annalisa PERISSA and other colleagues.

Engineering and Technical Support
Djilali ZIDANI, François SEVRE, Nicole LETOURNEUR, Jean-Pierre MICHEL, Sylvain CNUDDE and other colleagues.

School courses, lectures and lecturers, album of pictures, and other events
http://chalonge.obspm.fr